Review Article | Open Access

Soft Science

Lee et al. Soft Sci. 2026, 6, 46 DOI:10.20517/ss.2025.149

Wearable and implantable aptamer sensors for physiological monitoring

Hak Beom Lee[1], Daeho Lee[2,*], Seung Hwan Ko[1,*]

Keywords: Electrochemical aptamer-based sensor, biofluid monitoring, soft materials, wearable biosensors, continuous monitoring

Citation: Lee, H. B.; Lee, D.; Ko, S. H. Wearable and implantable aptamer sensors for physiological monitoring. *Soft Sci.* **2026**, *6*, 46. https://dx.doi.org/10.20517/ss.2025.149

Received: 28 Dec 2025 **First Decision:** 29 Jan 2026 **Revised:** 31 Mar 2026 **Accepted:** 14 Apr 2026 **Published:** 12 Jun 2026

Academic Editor: YongAn Huang **Copy Editor:** Shu-Yuan Duan **Production Editor:** Shu-Yuan Duan

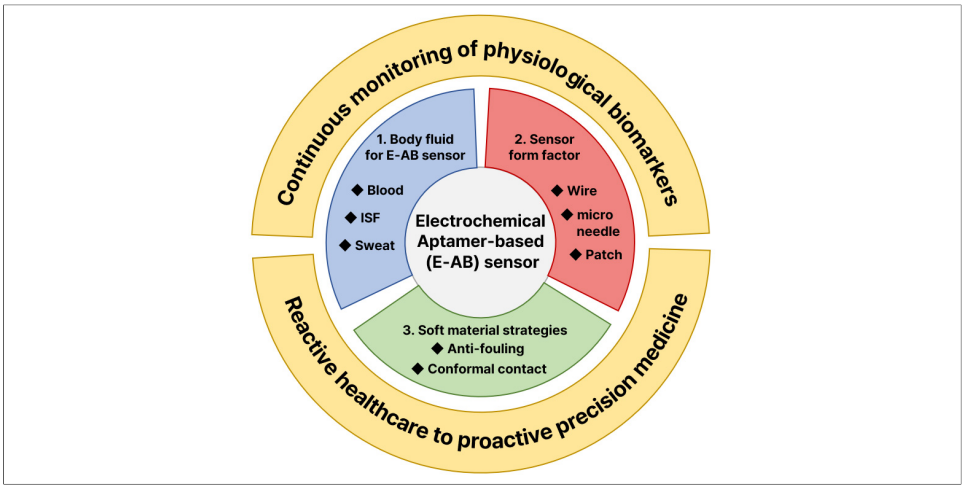

Abstract

The transition from reactive healthcare to proactive precision medicine necessitates technologies capable of real-time, continuous monitoring of physiological biomarkers. While enzymatic sensors have paved the way for metabolic tracking, they are intrinsically restricted to a narrow spectrum of redox-active analytes and often suffer from limited stability in complex biological environments. In contrast, electrochemical aptamer-based (E-AB) sensors have emerged as a revolutionary platform, offering a universal, reagent-free sensing mechanism driven by binding-induced conformational changes, independent of the target's chemical reactivity. This review provides a comprehensive analysis of the technological trajectory of E-AB sensors across the physiological continuum of biofluids: blood, interstitial fluid (ISF), and sweat. We critically examine distinct applications ranging from implantable wires for intravascular therapeutic drug monitoring and microneedle arrays for minimally invasive ISF analysis to wearable devices for non-invasive sweat sensing. A central theme of this work is the pivotal role of "soft material" strategies in facilitating the seamless integration of rigid electronics with soft biological tissues. We highlight how functional materials - including anti-fouling coatings, hydrogel interfaces, and flexible porous nanocomposites - bridge mechanical and chemical mismatches to mitigate biofouling and ensure stable, long-term bio-interfaces. Finally, we outline the remaining

[1]Department of Mechanical Engineering, Seoul National University, Seoul 08826, Republic of Korea.
[2]Department of Mechanical Engineering, Gachon University, Seongnam 13120, Republic of Korea.

[*]**Correspondence to:** Prof. Seung Hwan Ko, Department of Mechanical Engineering, Seoul National University, Seoul 08826, Republic of Korea. E-mail: maxko@snu.ac.kr; Prof. Daeho Lee, Department of Mechanical Engineering, Gachon University, Seongnam 13120, Korea. E-mail: dhl@gachon.ac.kr

hurdles for clinical translation, discussing strategies to achieve ultra-sensitivity, establish calibration-free methodologies, and integrate artificial intelligence (AI) for intelligent data processing, ultimately aiming for ubiquitous personalized healthcare.

INTRODUCTION

High-risk diseases such as cancer and stroke exhibit high morbidity and mortality rates globally, posing a severe threat to human health[1-3]. Since these diseases often present with non-specific symptoms, early detection is challenging, and establishing precision treatment strategies is essential due to individual variability in drug response[4]. Consequently, the paradigm of modern healthcare is shifting beyond reactive treatment toward proactive, preventive medicine based on the continuous collection of physiological data.

Recently, "Liquid Biopsy", which analyzes circulating nucleic acids, proteins, and exosomes in the blood, has garnered significant attention as an innovative technology[5,6]. According to guidelines from the National Academy of Clinical Biochemistry (NACB), blood contains various tumor markers [e.g., Carcinoembryonic antigen (CEA), Cancer antigen 125 (CA125)] and inflammatory biomarkers [e.g., C-reactive protein (CRP), tumor necrosis factor-α (TNF-α)], providing critical clues for disease diagnosis[7-10]. However, current gold-standard methods like Enzyme-linked immunosorbent assay (ELISA) are costly and labor-intensive, severely limiting their accessibility in resource-limited settings [Low- and middle-income countries (LMICs)][11,12]. Therefore, developing accessible Point-of-Care Testing (POCT) platforms remains an urgent priority.

Technologies capable of continuous or semi-continuous measurement already exist for a small number of metabolites, such as glucose[13] and lactate[14], and neurotransmitters like dopamine[15,16], serotonin[17], glutamate[18], and acetylcholine[19]. However, these approaches rely heavily on the specific chemical reactivity of the target (e.g., redox chemistry or enzymatic oxidation). Due to this dependence on reactivity, these techniques cannot be generalized to sense many other physiologically and clinically relevant molecules, leaving a significant unmet need for strategies that support continuous sensing independent of target reactivity.

Unfortunately, realizing this goal faces severe technical barriers[20,21]. First, to support continuous measurement, sensors must not rely on batch processing steps such as washing or separation. Second, for *in-vivo* applications, sensors must function without externally added reagents and maintain stability during prolonged exposure to blood or interstitial fluids. Conventional methods like chromatography or immunoassays require complex multistep batch processes, rendering them unsuitable for continuous sensing. Conversely, label-free sensors such as Surface Plasmon Resonance (SPR), Quartz Crystal Microbalance (QCM), and Field-Effect Transistors (FET) support continuous operation but often fail in blood (and by extension, *in-vivo*) because they cannot distinguish between specific target binding and the non-specific adsorption of proteins and cells[22-25].

In contrast, electrochemical aptamer-based (E-AB) sensors demonstrate the capability to support direct, continuous, real-time measurements *in-vivo*, serving as a platform independent of the target's chemical reactivity[26]. E-AB sensors utilize an aptamer labeled with a redox reporter attached to an electrode; upon binding to a specific target, the aptamer undergoes a conformational change that alters the electron transfer rate between the reporter and the electrode surface[27] [Figure 1A]. This reversible signal transduction mechanism enables continuous, selective, and reagent-free measurements suitable for diverse targets, including pharmaceuticals[26,28,29], drugs of abuse[30], proteins[31-33], and amino acids[26,31,34-36]. Indeed, E-AB

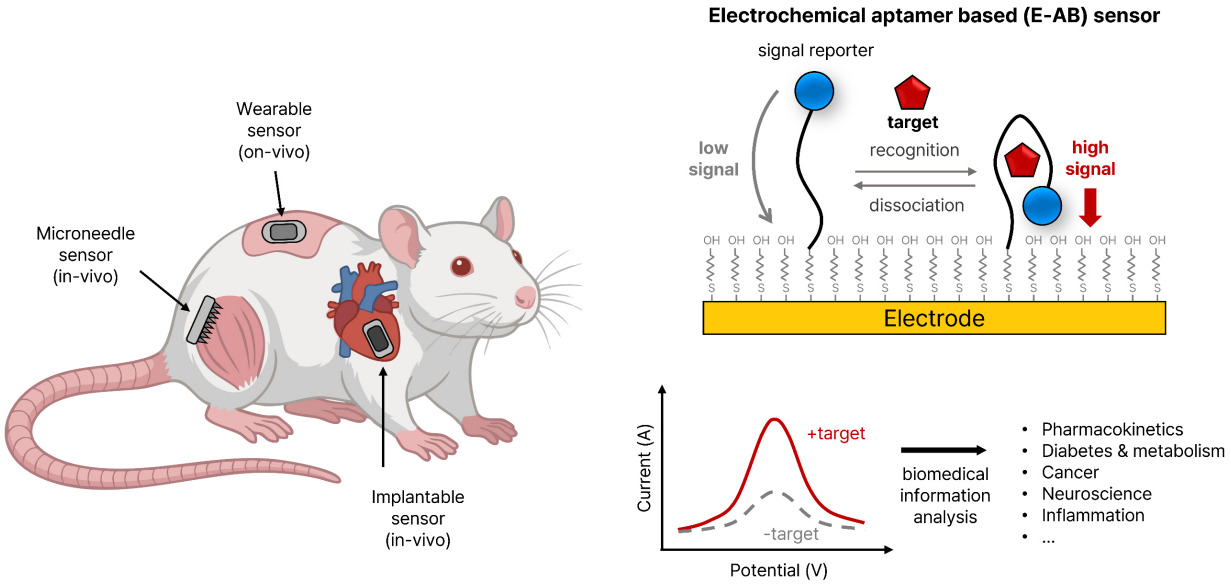

Figure 1. Overview of *in-vivo* & on-body E-AB sensor. E-AB: Electrochemical aptamer-based.

sensors have proven their utility in living animal models by enabling real-time monitoring of various drugs and metabolites, and even facilitating feedback-controlled closed-loop drug delivery via real-time target quantification[28,37].

This review examines the translation of E-AB sensor technology from the benchtop to the physiological biofluid continuum: 'Blood - Interstitial Fluid (ISF) - Sweat'. While blood serves as a rich information source, it entails risks associated with phlebotomy[38]. ISF has emerged as a compelling alternative, offering valuable insights into cancer progression via tumor-derived metabolites[39,40] and allowing for minimally invasive access. Furthermore, sweat offers a route for completely non-invasive monitoring, though challenges regarding biomarker variability remain[41].

Critically, this paper highlights Soft Material strategies as key enablers for achieving seamless mechanical and chemical integration between sensor systems and the human body. Functional material technologies that bridge mechanical mismatches and inhibit biofouling are essential requirements for accelerating the clinical translation of E-AB sensors. We analyze recent E-AB sensing applications across different biofluids and discuss future research directions for commercialization, including the attainment of high sensitivity and specificity, and the establishment of calibration-free systems.

FUNDAMENTAL CONSIDERATIONS FOR *IN-VIVO* AND ON-BODY SENSING

Whole blood, ISF, and sweat do not exist as isolated biological compartments; rather, they function as an interconnected continuum regarding the migration path of analytes. Typically, biomolecules originate in the circulatory system, partition across the capillary barrier into the ISF, and ultimately permeate the sweat glands for excretion onto the skin surface. This trajectory is governed by a complex interplay of passive diffusion and diverse active transport mechanisms[42,43] [Figure 2A].

Within this physiological sequence, ISF can be characterized as a fluid derived from its systemic progenitor, blood. The dense capillary network within the dermis serves as the primary gateway for solute propagation into the tissue, resulting in the presence of a vast majority of blood-borne analytes within the ISF[44-46]. Consequently, the efficiency of mass transport across these capillary boundaries is the primary determinant of the solute concentration and compositional profile of the ISF[1,47,48].

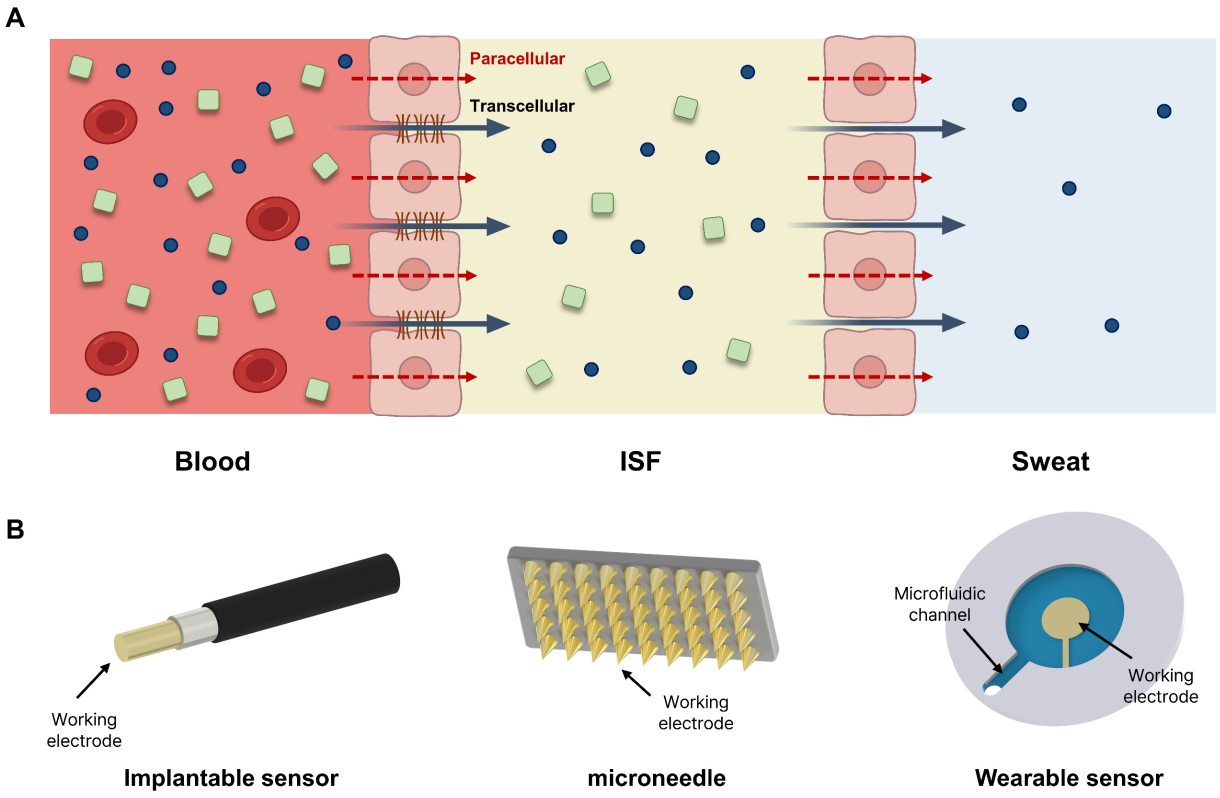

Figure 2. Schematic illustration of biomarker partitioning across biofluid compartments and corresponding electrochemical sensing modalities. (A) Schematic of biomarker transport pathways (red arrows: paracellular, black arrows: transcellular) and analytes (blue circles: small molecules, green squares: larger analytes) across blood, ISF, and sweat compartments; (B) Illustrations of implantable, microneedle, and wearable electrochemical sensors. ISF: Interstitial fluid.

Analyte transfer from the vasculature to the interstitium is a highly selective permeation process rather than random distribution. It is strictly regulated by the structural properties of endothelial cells and the physicochemical attributes of the analytes, specifically molecular weight, charge, and polarity. Transport pathways are broadly categorized into paracellular and transcellular routes. Molecular size acts as a predominant filter; inter-endothelial junctions (IEJs), composed mainly of cadherins and tight junctions, regulate this flow. Small molecules (under 3 kDa) diffuse freely through cadherin junctions regardless of charge[2,49]. Conversely, intermediate-sized molecules (3-70 kDa) face partial restriction by tight junctions, necessitating a combination of paracellular and transcellular transport[3]. Furthermore, transport mechanisms diverge based on charge state and polarity[50,51]. For instance, while hydrophobic molecules can permeate directly across the plasma membrane via simple diffusion, hydrophilic macromolecules typically require active endocytosis and subsequent vesicular transport to traverse the cellular barrier[52].

Ultimately, ISF functions as a reservoir for blood-derived constituents that have successfully navigated these selective barriers. These solutes subsequently enter the sweat glands, driven by concentration gradients or active secretion mechanisms, to establish the final composition of sweat. Therefore, a fundamental comprehension of sweat and ISF biosensing requires a prior understanding of the dynamic partitioning mechanisms that govern analyte progression from whole blood through each biological barrier.

Blood

Whole blood serves as a critical biological specimen containing essential data for monitoring overall physiological conditions. Although the majority of target biomolecules, including proteins, ions, and metabolites, are dissolved within the plasma[53], the capability to detect these targets directly in a whole blood

environment is a prerequisite for the application of implantable sensors as emphasized in the introduction.

Once a sensor is introduced into the body, endogenous biological materials rapidly accumulate on its surface, a phenomenon termed "fouling". This adsorption cascade initiates with water molecules, followed immediately by ions which establish an electrical double layer[54]. Subsequently, various proteins begin to adsorb based on their specific diffusivity and surface affinity, a process that eventually leads to the attachment of cellular components[54].

In particular, high-abundance proteins in the blood, such as Albumin, Immunoglobulin G (IgG), and Fibrinogen, rapidly coat the electrode surface. This protein layer physically impedes the conformational changes required for aptamer function and blocks electron transfer pathways, thereby significantly diminishing the sensor's activation window[55,56].

Furthermore, this adsorbed protein layer triggers the adhesion and aggregation of platelets. Through complex protein-cell interactions, platelet aggregates cross-link with fibrin to generate thrombi on the electrode surface. Thrombus formation is a critical safety hazard that extends beyond mere sensor performance degradation, as it can lead to vascular occlusion or embolism[57-59]. Although pharmaceutical interventions are employed to manage thrombosis, these drugs carry their own risks of complications; therefore, thrombogenicity must be viewed as a safety issue rather than solely a sensor longevity problem[60,61].

In addition to thrombosis, the protein-conditioned surface facilitates bacterial colonization, leading to the development of a biofilm[62]. Biofilms are composed of bacteria encased within a self-produced matrix of insoluble extracellular polymeric substances (EPS). This 3D EPS matrix not only stabilizes the biofilm structure but also significantly enhances bacterial resistance against antibiotics and the host immune system. The biofilm matures as bacteria proliferate and EPS accumulates[63,64]. The most frequently identified pathogens associated with blood-contacting devices are coagulase-negative Staphylococcus, followed by Pseudomonas aeruginosa. Infections associated with biofilms can be up to 75% more prevalent than those caused by planktonic bacteria and exhibit substantial resistance to both immune responses and systemic antibiotic therapies. Consequently, biofilm-mediated infections are notoriously difficult to eradicate and have a profound negative impact on patient health and quality of life[65,66].

Interstitial fluid

Interstitial fluid (ISF), generated via the filtration of systemic blood, has emerged as a compelling target fluid for biosensor applications. While ISF is largely devoid of cellular components such as erythrocytes and platelets that typically induce severe biofouling in whole blood, it retains a rich profile of cellular metabolites and clinically relevant biomarkers[67-69]. Significant analytes identified in ISF include protein biomarkers such as CA-125, HER2, and PSA which present the possibility of cancer such as ovarian, breast and prostate cancer[70,71], as well as nucleic acid markers including microRNAs (e.g., miR-10b, 21, 155, 16)[72] and exosomes[73,74]. The utility of ISF lies in its compatibility with direct analysis without extensive pretreatment, offering a minimally invasive alternative to conventional biofluids like blood, urine, or saliva for disease diagnosis, prevention, and therapeutic monitoring[75-77].

However, the matrix of ISF presents its own set of stability challenges. Although less aggressive than whole blood, ISF is susceptible to fouling through the non-specific adsorption of proteins and lipids. These contaminants can compromise sensor integrity, for instance, by accelerating the desorption of alkylthiolate self-assembled monolayers (SAMs), thereby shortening the operational lifespan of the device[78]. Furthermore, biological degradation poses a distinct threat; ISF is not devoid of nucleases, meaning that sensing elements such as aptamers are vulnerable to enzymatic degradation rather than simple physical

fouling[79]. Consequently, robust anti-fouling strategies remain a prerequisite for ISF-based sensors, mirroring the requirements for whole blood analysis.

A critical consideration in evaluating ISF for diagnostics is establishing the correlation between analyte concentrations in ISF versus whole blood. The distribution of target molecules in ISF is governed by their physicochemical properties, such as size and charge state, often resulting in lower concentrations compared to the bloodstream. Specifically, medium-sized, negatively charged molecules (3-70 kDa) face a transport barrier imposed by the negatively charged glycocalyx lining the luminal surface of the vascular endothelium. This electrostatic repulsion significantly impedes the partitioning of such analytes into the interstitial space[80].

In addition to concentration discrepancies, temporal dynamics, or "lag time", must be considered for small hydrophilic molecules. For instance, glucose monitoring in ISF typically exhibits a measurement delay of 20-35 min relative to blood glucose levels due to transport kinetics[81]. However, this latency is not universal; certain small hydrophilic and hydrophobic species are known to reach equilibrium between blood and ISF relatively rapidly[76].

Conversely, the localized nature of ISF generation offers a distinct advantage: since ISF composition is heavily influenced by neighboring cells, it can contain significantly higher concentrations of disease-specific biomarkers than systemic circulation. Notably, biomarker concentrations within the ISF of a tumor microenvironment can exceed systemic blood levels by three orders of magnitude (1,000-1,500 times), providing superior sensitivity for localized pathology detection[82].

Sweat

Sweat serves as a premier biofluid for continuous, non-invasive biomarker monitoring, distinguishing itself by the vast availability of sampling sites across the epidermis and its inherent accessibility[83,84]. Furthermore, when a sensor interface is properly sealed against skin, it creates an isolated microenvironment. This configuration effectively shields the sensing area from external fluids and contaminants, mitigating fouling issues typically associated with *ex-vivo* detection.

However, the passive nature of perspiration poses a significant challenge; without a continuous secretory flow, stagnant sweat may accumulate within the sensor interface, exacerbating contamination artifacts originating from the skin surface[85]. To prevent the compromise of real-time monitoring capabilities, active stimulation via iontophoresis is frequently employed. This technique utilizes electrical current to deliver pilocarpine into the localized dermis, agonizing muscarinic receptors within the sweat glands to induce secretory activity[86,87]. While perspiration can also be triggered by thermal, physical, or psychological stimuli - each resulting in slightly varying fluid compositions[42] - this study primarily focuses on iontophoresis-mediated generation to ensure controlled parameters for sensor design.

As an excretory fluid, sweat exhibits a broad range of salinity, typically fluctuating between 10 and 100 mM[83]. Such variations in ionic strength can fundamentally alter the thermodynamics governing the binding-induced conformational switching that drives signaling in E-AB sensors[88]. Consequently, compensatory mechanisms using ion-selective electrodes may be requisite. Additionally, dynamic pH shifts (spanning 4.5 to 7.0) can distort the concentration readouts of weak acids and bases[83]. For instance, exercise-induced sweat often manifests with lower pH, variable electrolyte profiles, and susceptibility to dilution. Conversely, naturally secreted sweat, characterized by extremely low flow rates, is highly vulnerable to evaporation and cutaneous contamination. Therefore, rigorous control over sweat collection dynamics is critical to ensure analytical accuracy[42].

From a mass transport perspective, sweat generally presents lower biomarker concentrations than blood or ISF due to filtration mechanisms. Transport pathways are strictly governed by molecular properties: small hydrophobic species (e.g., steroid hormones and many drugs) readily traverse the epithelium via transcellular diffusion. In contrast, small hydrophilic solutes (e.g., metabolites) are relegated to the more restrictive and dilution-prone paracellular entry path[42]. Macromolecules, such as proteins, are hypothesized to migrate via a combination of paracellular transport and transcytosis[42,43], undergoing significant filtration; albumin, for instance, is diluted by at least three orders of magnitude relative to blood[89]. Consequently, biomarkers present at pM levels in circulation are exceptionally difficult to quantify in sweat[43,86].

Despite these limitations, certain analytes demonstrate high clinical utility. Glucose levels, for instance, appear largely decoupled from sweat generation rates and exhibit trends correlating with blood glucose[85,90]. Similarly, cortisol, a marker for acute and chronic stress, shows a concentration difference of roughly one order of magnitude between blood and sweat, making it a viable target for sweat-based detection[91]. However, complications persist with analytes like lactate, which is generated endogenously by the sweat gland metabolism, thereby reducing its correlation with systemic levels[42,92]. Collectively, while promising, sweat-based biomarker detection faces distinct physiological hurdles compared to blood or ISF analysis.

Beyond the physicochemical properties of the biofluids themselves, the continuum framework also dictates specific requirements for aptamer selection. Aptamers deployed in blood must prioritize nuclease resistance and selectivity within high-protein matrices, motivating the use of chemically modified backbones such as 2′-O-methyl RNA[93]. In ISF, where analyte flux across the dermis is limited, high-affinity (low K_D) aptamers are preferred to maximize productive binding events per available target molecule[94], alongside truncated sequences tailored for microneedle geometries[95,96]. Finally, in sweat, the wide fluctuations in ionic strength (10-100 mM) and pH (4.5-7.0) can readily destabilize aptamer secondary structures, necessitating sequences with highly robust folding thermodynamics[97]. Ultimately, these biofluid-specific aptamer requirements are an inseparable component of the continuum sensing design framework discussed throughout this review.

Scope of biofluids for continuous E-AB monitoring: opportunities and limitations

As discussed in the preceding subsections, blood, ISF, and sweat currently represent the most viable physiological mediums for realizing real-time, continuous monitoring using E-AB sensors. Blood provides the gold standard for direct therapeutic drug monitoring (TDM), while ISF and sweat offer minimally invasive (via microneedle arrays) and non-invasive (via epidermal patches) alternatives, respectively. A shared, critical characteristic of these three biofluids is their physical compatibility with continuous sensor integration.

While other biofluids, most notably urine and saliva, are undeniably valuable for conventional clinical diagnostics, they present fundamental physiological and engineering barriers to the continuous, *in-situ* monitoring framework targeted in this review. Urine, for instance, is inherently intermittent in its external availability, which fundamentally precludes the continuous, real-time tracking that wearable or implantable E-AB sensors aim to achieve. Furthermore, the renal filtration process substantially alters biomarker concentrations relative to systemic circulation, potentially diminishing physiological fidelity for real-time dynamic tracking[98,99].

Similarly, although saliva is a non-invasive fluid, intraoral sensor integration is hindered by severe mechanical and user-compliance limitations. More critically from an electrochemical perspective, the oral environment induces rapid and aggressive biofouling due to pellicle formation and bacterial biofilm metabolites, which can compromise the binding-induced conformational changes of aptamers within hours.

Table 1. Comparison of biofluids for continuous E-AB sensor applications

Biofluid	Key merits & characteristics	Shortcomings (Limitations)	Engineering challenges for E-AB sensors
Blood	Gold standard for therapeutic drug (TDM)[162] Contains the majority of systemic target biomolecules (proteins, ions, metabolites)[132]	High abundance of proteins (Albumin, IgG, Fibrinogen)[185,186] Risk of thrombosis (platelet aggregation and fibrin cross-linking)[187,188]	Severe biofouling blocking electron transfer and aptamer changes[186] Preventing device-associated biofilm formation[189,190] Managing thrombogenicity as a safety hazard[187]
ISF	Minimally invasive continuous monitoring[69,80,117,123] Devoid of large cellular components (erythrocytes, platelets)[117,191,192] Can contain highly concentrated localized biomarkers (e.g., up to 1,500X in tumors)[193]	Temporal lag time (e.g., 20-35 min for glucose) compared to blood[81] Concentration barriers for medium-sized/negatively charged molecules (due to glycocalyx)[185,194] Presence of nucleases [93]	Preventing enzymatic degradation of aptamers by nucleases[93] Mitigation non-specific adsorption of proteins and lipids that compromises SAMs[177]
Sweat	Non-invasive and broadly accessible across the epidermis[195,196] Sealed sensor interface can prevent external *ex-vivo* contamination[97,141]	Requires active stimulation (e.g., iontophoresis) due to stagnant flow[97,141] Macromolecules (e.g., albumin) are highly diluted via filtration barrier[43] Endogenous generation (e.g., lactate) lowers systemic correlation[197]	Compensating for dynamic pH shifts (4.5-7.0) and salinity (10-100 mM) affecting E-AB thermodynamics [94,195] Preventing evaporation and cutaneous contamination[43]
Urine	Value for conventional clinical diagnostics[198]	Inherently intermittent availability, fundamentally precluding continuous real-time tracking[198] Renal filtration substantially alters physiological fidelity relative to blood[99]	Not viable for the uninterrupted, continuous *in-situ* monitoring framework[99,198]
Saliva	Non-invasive diagnostic value	Inconsistent correlation with blood analyte concentrations depending on environment[199] Intraoral integration faces severe mechanical and user-compliance limitations[200]	Overcoming rapid/aggressive biofouling from pellicle and bacterial biofilms[200] Mitigating electrochemical interference from complex matrix (proteins, mucins, food)[199]

E-AB: Electrochemical aptamer-based; TDM: therapeutic drug monitoring; ISF: interstitial fluid; SAM: self-assembled monolayer; IgG: Immunoglobulin G.

The complex salivary matrix, rich in proteins, mucins, and food residues, introduces significant electrochemical interference. Moreover, the correlation between salivary and blood analyte concentrations often remains inconsistent and highly dependent on environmental factors[100-102].

Therefore, to maintain a cohesive focus on technologies capable of uninterrupted, long-term continuous monitoring and their associated material engineering challenges, the primary scope of this review is intentionally directed toward E-AB sensor platforms designed for blood, ISF, and sweat. Nevertheless, to provide a comprehensive perspective for future sensor designs, a comparative analysis of the merits, shortcomings, and key engineering challenges associated with these five distinct biofluids is summarized in Table 1.

IN-VIVO E-AB SENSOR

Implantable blood analysis applications using wire-based E-AB sensor

For real-time drug monitoring within the bloodstream of live animal models, the sensor's form factor is a critical determinant of success. Consequently, implantable E-AB sensors have predominately adopted a wire-based electrode configuration [Figure 2B]. This prevalence is due to the wire geometry being structurally optimal for intravascular insertion and deep tissue penetration while ensuring minimal invasiveness during deployment[103].

Studies involving the implantation of sensors into the vasculature and tissues of live rats have substantiated the clinical validity of E-AB sensors[28] [Figure 3A]. Notably, continuous tracking of *in-vivo* pharmacokinetics

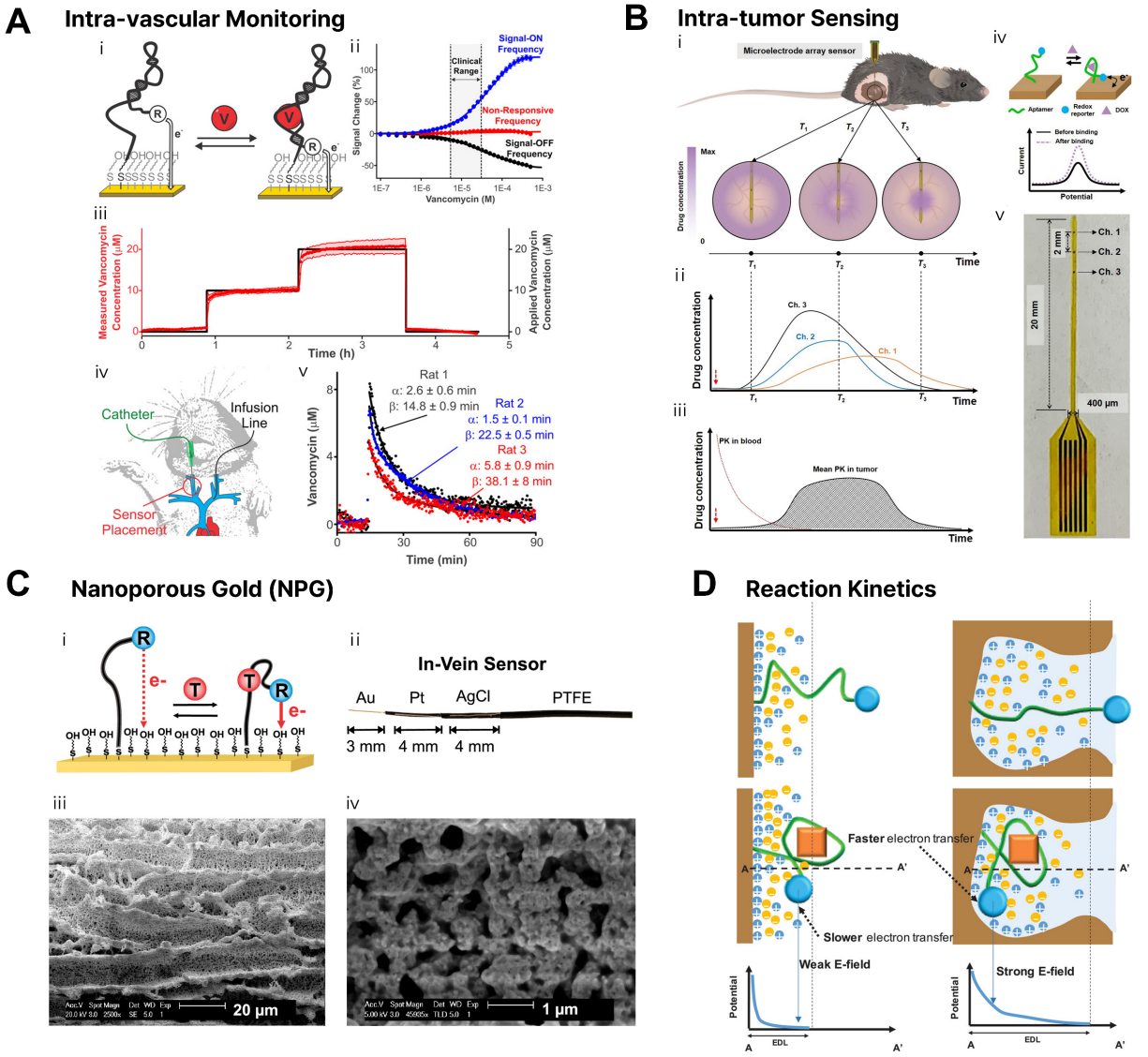

Figure 3. Wire-based implantable E-AB sensor platforms and sensing mechanisms. (A) Intra-vascular monitoring. Reprinted with permission[28]. Copyright 2019, American Chemical Society; (B) Intra-tumor sensing. Reprinted with permission[105]. Copyright 2022, American Association for the Advancement of Science; (C) Nanoporous Gold (NPG) configuration and SEM images. Reprinted with permission[107]. Copyright 2021, American Chemical Society; (D) Conceptual illustration of reaction kinetics. Reprinted with permission[106]. Copyright 2021, John Wiley and Sons. PK: Pharmacokinetic; PTFE: polytetrafluoroethylene; E-AB: electrochemical aptamer-based; SEM: scanning electron microscope.

has been successfully achieved in the veins of awake, ambulatory animals without the need for anesthesia[26]. This methodology represents a significant evolution from earlier strategies that relied on *ex-vivo* microfluidic devices utilizing stacked laminar flows to prevent whole blood contact[104]. By coating the sensor with a biocompatible polymer membrane to minimize fouling effects in whole blood, researchers have enabled stable monitoring in freely moving subjects (Note: Fouling shielding mechanisms are detailed in the subsequent section; this section focuses on the review of real-time *in-vivo* measurement outcomes). This approach provides precise physiological data by eliminating stress factors associated with anesthesia. Furthermore, the versatility of E-AB sensors has been confirmed through the successful detection of various distinct drugs, including doxorubicin, kanamycin, gentamicin, and tobramycin. Expanding beyond the bloodstream, the T. Soh research group demonstrated the utility of E-AB sensors for monitoring drug concentrations within tumor tissues, offering a new direction for drug design by analyzing chemotherapeutic efficacy as a function of tissue depth[105] [Figure 3B].

While miniaturizing electrodes to the micrometer scale is essential for intravascular insertion, such reduction inherently decreases the physical surface area, leading to a degraded signal-to-noise (S/N) ratio and reduced utility for molecular diagnostics[106]. To overcome this trade-off, extensive research has focused on maximizing the effective electrode surface area using Nanoporous Gold (NPG)[107-111]. NPG leverages a 3D nanostructure to dramatically increase the effective surface area relative to the geometric area, thereby securing sufficient electrochemical signals even in miniaturized sensors[107,108]. Building on initial designs that increased microscopic surface area via surface roughening[111], the Plaxco team successfully amplified the methylene blue redox signal by approximately 25-fold. This was achieved by employing cyclic voltammetry for the alternating deposition and stripping (alloying/dealloying) of zinc (Zn), which increased the microscopic surface area of the wire by up to 100-fold[107] [Figure 3C]. Moreover, it has been proven that nanostructured electrodes improve sensor sensitivity and reaction kinetics not merely by increasing area, but by accelerating electron transfer rates due to reduced charge screening effects[106,111] [Figure 3D]. Additionally, the pore size and morphology of the NPG thin film directly influence sensor performance by dictating analyte accessibility. It has been observed that the optimal signaling frequency varies depending on the film morphology. By creating libraries of various NPG morphologies to identify optimal structures, the signaling efficiency of nucleic acid-based biosensors can be optimized[108,110]. Electrochemical roughening processes are also presented as an effective method for fabricating high-surface-area electrodes[111].

Implantable ISF analysis applications using microneedle-based E-AB sensor

Monitoring ISF located beneath the epidermis has emerged as a promising alternative to blood-based monitoring. ISF contains physiological information analogous to blood yet remains accessible via microneedles in a minimally invasive manner. Recent advancements have integrated E-AB technology into these microneedle platforms, evolving them into systems capable of real-time, reagent-free detection of specific analytes. Currently, the most successful implementation of microneedle-based sensors is the Continuous Glucose Monitoring (CGM) device. Commercialized by companies such as Dexcom, this technology enables the continuous tracking of glucose levels in ISF through microscopic needles[112-114]. However, to transcend the limitations of enzymatic sensors and detect a broader range of drugs and biomarkers without reagents, recent research is increasingly pivoting toward incorporating E-AB technology into microneedle platforms[115] [Figure 4A].

A primary application of microneedle E-AB sensors is TDM for pharmaceuticals with narrow therapeutic windows. For instance, studies have reported the successful acquisition of pharmacokinetic (PK) profiles by attaching 3D-printed microneedle sensor arrays to live rats to measure drug concentrations in ISF in real-time[95,116,117]. Specifically, for antibiotics requiring precise dosage control, microneedle E-AB patch modules have been designed to achieve high-resolution sensing[95] [Figure 4B]. These technologies successfully differentiated and detected representative antibiotics such as tobramycin and vancomycin within their respective therapeutic ranges of 4-21 μM and 6-35 μM in an ISF environment. Furthermore, recent developments include hyaluronic acid-based hydrogel microneedles integrated with flexible electrodes. These systems allow for the simultaneous precision detection of antibiotics and colorimetric monitoring of pH changes at infection sites, thereby providing a comprehensive evaluation of therapeutic efficacy[118] [Figure 4C].

The scope of application is expanding beyond drugs to include metabolites and hormone monitoring. A technology termed the 'Wearable Aptalyzer', based on methacrylated hyaluronic acid (MeHA) hydrogel microneedle arrays, successfully tracked glucose and lactate levels in the dermal ISF of live diabetic rats via daily electrochemical measurements over a three-day period[96]. Notably, this study confirmed the multiplexing potential of E-AB sensors for metabolic disease management by maintaining stable simultaneous detection without severe biofouling. Additionally, sensor arrays for the continuous real-time

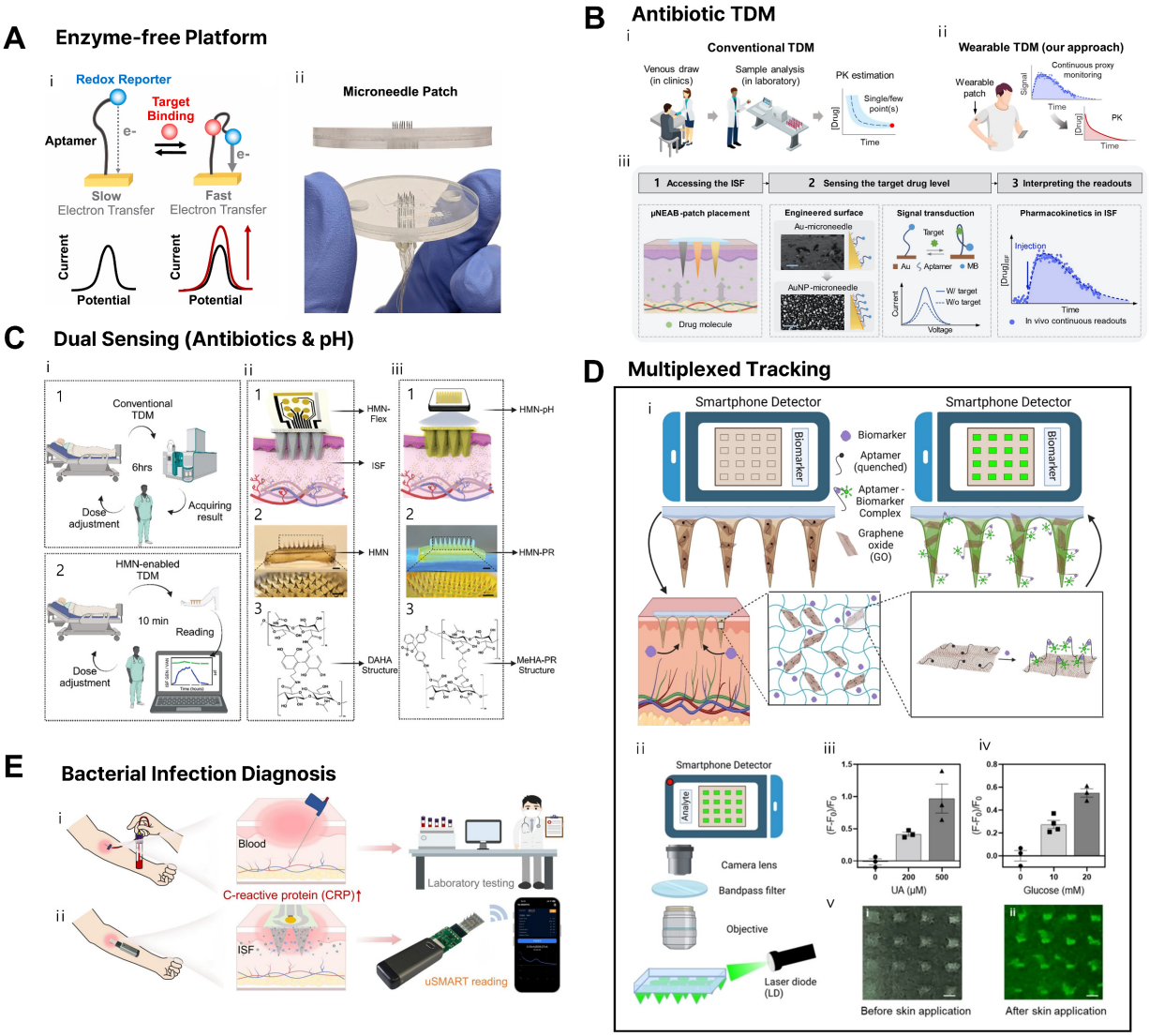

Figure 4. Microneedle-based implantable E-AB sensor platforms and sensing mechanisms. (A) Wearable microneedle-based E-AB sensor schematic. Reprinted with permission[115]. Copyright 2023, Elsevier; (B) Conventional and wearable TDM comparison, with μNEAB-patch illustration and process flow. Reprinted with permission[95]. Copyright 2022, American Association for the Advancement of Science; (C) Dual-sensing microneedle platforms: HMN-Flex and HMN-pH. Reprinted with permission[118]. Copyright 2024, John Wiley and Sons; (D) Point-of-care biosensing strategy for multi-analytes. Reprinted with permission[121]. Copyright 2023 John Wiley and Sons; (E) μSMART system for CRP detection. Reprinted with permission[122]. Copyright 2025, American Chemical Society. TDM: Therapeutic drug monitoring; ISF: interstitial fluid; MB: methylene blue; HMN: hydrogel microneedle; HMN-RR: hydrogel microneedle-phenol red; DAHA: dopamine-based hyaluronic acid; CRP: C-reactive protein; E-AB: electrochemical aptamer-based.

monitoring of L-Tryptophan, a key amino acid linked to depression[119], and technologies detecting the stress hormone cortisol transdermally using conductive microneedles[120], are extending the domain of healthcare into mental health management.

Building on the same MeHA hydrogel microneedle platform, the same research group demonstrated a versatile point-of-care biosensing strategy by integrating graphene oxide-nucleic acid (GO·NA) probes directly within the hydrogel matrix[121] [Figure 4D]. Upon skin insertion, ISF diffuses into the swollen microneedles, whereupon target binding induces aptamer conformational changes that dissociate the aptamer-graphene oxide complex and restore fluorescence in a reagentless, turn-on manner. This approach was validated across four analytes (glucose, uric acid, insulin, and serotonin) spanning both small molecules

and proteins, with *ex vivo* accuracy confirmed alongside a portable fluorescence reader for on-site use. Together with the electrochemical Wearable Aptalyzer, these studies illustrate that hydrogel microneedle-aptamer platforms can be adapted across orthogonal transduction modalities to meet diverse clinical monitoring needs.

E-AB sensors are also being utilized for diagnostic purposes, particularly for bacterial infections. An integrated aptasensing platform based on methacrylate hyaluronic acid sensor design has been reported, which allows for the immediate, reagentless, on-site monitoring of specific bacterial infections such as S. aureus and the assessment of treatment responses[122] [Figure 4E]. Beyond bacterial infections, E-AB sensors are applicable to allergy diagnosis. Microneedle E-AB sensors capable of detecting IgE antibodies through the skin have opened new avenues for easily diagnosing food allergy sensitization without the need for blood draws[123].

In conclusion, microneedle E-AB sensors have progressed beyond animal models to the stage of continuously monitoring molecules within human dermal ISF[124]. Although challenges such as limited ISF flow rates and biological responses remain, multifaceted material and structural innovations - such as the adoption of 3D printing processes[116] and functionalization using hydrogels[118] - are solidifying their potential as next-generation continuous monitoring platforms.

Soft materials for anti-fouling

To ensure that E-AB sensors function without losing signal accuracy in complex biofluids, designing an interface based on “soft materials” to protect the electrode surface from fouling is essential. An ideal anti-fouling surface should be hydrophilic, act simultaneously as a hydrogen bond donor and acceptor, and possess electrically neutral characteristics[103] [Figure 5A]. These molecular properties, realizable on gold electrodes via Self-Assembled Monolayers (SAMs), facilitate the strong binding of water molecules to the surface, creating a highly hydrated layer that serves as an effective "water barrier" against contaminant adsorption. Furthermore, increasing the packing density of surface molecules is a critical factor in maximizing hydrogen bonding to enhance surface hydration[125].

Beyond fouling prevention, tuning surface charge is an effective strategy for enhancing selectivity toward target analytes. In cases where structurally similar drugs (e.g., aminoglycosides) must be distinguished, tuning the surface charge using mixed SAMs can exclude interference via electrostatic repulsion[126,127] [Figure 5B]. Additionally, optimizing the chemical structure of SAM end-groups or introducing zwitterionic moieties aids in maintaining the chemical stability of the monolayer itself within biological fluids[128-130].

However, as monolayer-level control alone is insufficient to fully overcome harsh *in-vivo* environments, soft coating strategies utilizing functional polymers have recently emerged as key solutions[131] [Figure 5C]. Notably, introducing hydrophilic polymers such as polyethylene glycol (PEG) is a powerful method for extending sensor lifespan. Chen *et al.* designed a NPG electrode mimicking the structure of intestinal villi and applied a PEG-based coating to effectively protect the sensor surface[132]. This approach successfully suppressed baseline drift and dramatically improved signal stability[132]. Through this protective coating, the sensor achieved a breakthrough result: it maintained robust sensitivity for kanamycin in undiluted human serum *in vitro* over four weeks with intermittent sampling at specific days. Furthermore, the system demonstrated exceptional *in-vivo* translation, sustaining its continuous sensing functionality for up to one week when implanted within the femoral vein of free-moving rats.

In addition to PEG, the application of 3D polymer networks, such as hydrogels, as physical barriers completes the sensor’s durability [Figure 5D]. The presented biocompatible hydrogel coating technology maximizes the advantages of soft materials in a similar context to PEG coatings. Hydrogels physically block

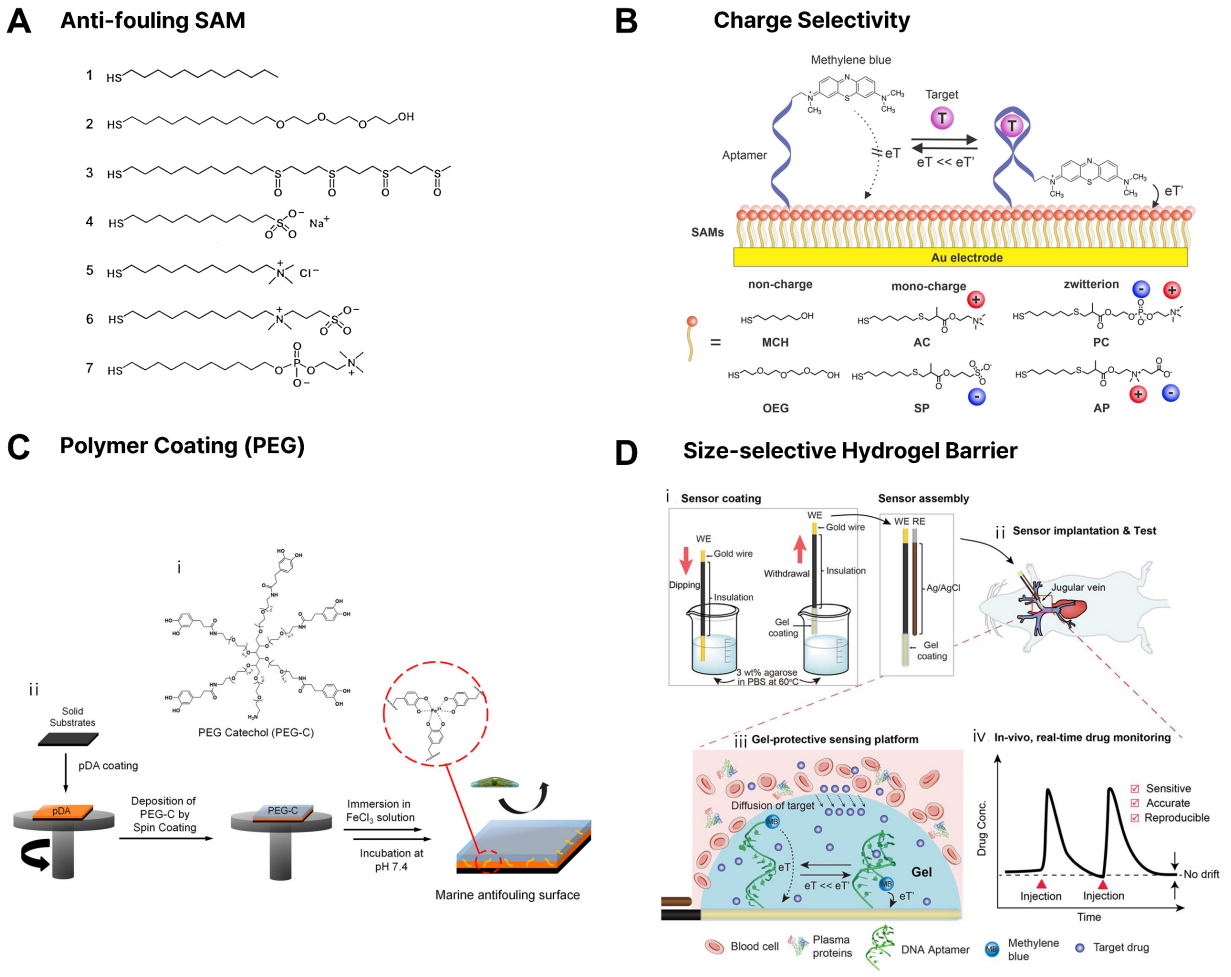

Figure 5. Soft material strategies for anti-fouling and long-term stability of E-AB sensors. (A) Anti-fouling SAM. Reprinted with permission[103]. Copyright 2001, American Chemical Society. (B) Charge selectivity. Reprinted with permission[128]. Copyright 2021, American Chemical Society. (C) Polymer coating (PEG). Reprinted with permission[131]. Copyright 2018, American Chemical Society. (D) Size-selective hydrogel barrier. Reprinted with permission[133]. Copyright 2023, American Chemical Society. MCH: 6-mecapto-1-hexanol; AC: ammonium choline; PC: phorsphorycholine; OEG: oligoethylene glycol; SP: sulfopropylmethacrylate potassium; AP: ammonio propionate; WE: working electrode; PBS: phosphate buffered saline; E-AB: electrochemical aptamer-based; SAM: self-assembled monolayer.

the access of large enzymes, such as proteins present in the blood, thereby preventing aptamer degradation and inhibiting fouling. At the same time, they allow the free diffusion of small drug molecules, enabling stable, long-term continuous drug monitoring across multiple *in-vivo* sites, including blood vessels and tissues[133]. Thus, soft material technologies like PEG and hydrogels are essential protective measures for translating E-AB sensors from laboratory settings to real-world biological applications.

Furthermore, anionic polymer coatings such as Nafion act as charge-selective barriers. They repel negatively charged interfering species in the blood while selectively allowing the permeation of target molecules, thereby contributing to the improvement of the signal-to-noise ratio[134].

The sensors discussed above operate on the principle of direct immersion within the body, a strategy we term '*in-vivo*', characterized by intimate contact with internal biofluids such as blood and ISF. This architecture grants access to the richest molecular information but imposes the most stringent biological constraints: chronic biofouling from protein adsorption and cellular adhesion, thrombus formation on electrode surfaces,

and the mechanical demands of long-term tissue cohabitation. Together, these challenges necessitate the soft-material and anti-fouling strategies detailed in Section **Soft materials for anti-fouling.**

In contrast, the sensors described in the following section operate 'on-body', interfaced with the outer surface of the body rather than its interior. By confining the sensing interface to the skin surface and leveraging sweat as the sampling medium, this approach avoids the safety risks and surgical burden of implantation. The trade-off, however, is a fundamentally different set of constraints: lower and more variable biomarker concentrations due to filtration across biological barriers, intermittent and sweat-rate-dependent analyte delivery, and susceptibility to environmental contamination and motion artifacts. The soft-material strategies required here, such as breathable substrates, superwetting microfluidics, and adhesive biocomposites, are accordingly distinct from those demanded *in-vivo*.

ON-BODY E-AB SENSOR

Wearable sweat analysis applications using E-AB sensor

Recent breakthroughs in sweat monitoring sensor technology have paved the way for innovative real-time tracking of physiological states directly linked to human performance and health, such as dehydration, fatigue, and disease[90,97,135-140]. Sweat presents an attractive alternative to blood for analysis, offering non-invasive access with relatively lower risks of biofouling. However, the majority of existing wearable sensors rely on enzymatic sensing mechanisms, which inherently suffer from sensitivity to environmental factors like temperature and humidity, as well as limited long-term stability due to enzyme degradation. Consequently, E-AB sensors, known for their superior stability and selectivity, are emerging as a next-generation solution for sweat analysis.

A primary application of sweat-based E-AB sensors lies in the monitoring of stress and sex hormones. To non-invasively detect cortisol, a key biomarker of stress, skin-interfaced aptamer sensors integrated with FETs have recently been developed [Figure 6A]. These sensors demonstrate a wide dynamic range spanning from picomolar (pM) to micromolar (μM) levels. Through the standardized Trier Social Stress Test (TSST), researchers have successfully validated the correlation between sweat and salivary cortisol levels, proving the sensor's reliability in biofluid environments[141]. Furthermore, Ye *et al.* has pioneered personalized reproductive healthcare by developing a wearable sensor targeting estradiol[97]. This study stands as a landmark innovation, successfully detecting sub-nanomolar levels of hormones in human sweat, thereby demonstrating the feasibility of monitoring menstrual cycles via wearable E-AB technology.

E-AB sensors also exhibit exceptional performance in detecting small-molecule drugs and protein biomarkers that are challenging for enzymatic sensors. In the context of preventing drug abuse, sensor arrays have been reported to detect multiple illicit drugs in sweat with high sensitivity (hundreds of pM) while distinguishing between target drugs and interferents via distinct electrochemical fingerprints[142] [Figure 6B]. Expanding on this, multiplexed sensor arrays for monitoring multiple anticancer drugs (e.g., cyclophosphamide, cisplatin, and docetaxel) have been developed as a step toward personalized chemotherapy. While these systems demonstrated robust shelf-life stability over 15 days, their precise drug discrimination and quantification capabilities were validated using discrete measurements within artificial sweat *in vitro*[143], laying the groundwork for future continuous on-body tracking.

Beyond general health management, innovations in form factors are enabling the early detection of severe diseases. A smart ring sensor designed for atherosclerosis management simultaneously detects C-reactive protein (CRP), cholesterol, and potassium ions (K+), tracking patient trends via a mobile application[144]. Additionally, research on cytokine detection to prevent life-threatening inflammatory storms is gaining momentum. A system integrating a Janus membrane with a graphene-FET successfully detected cytokines in

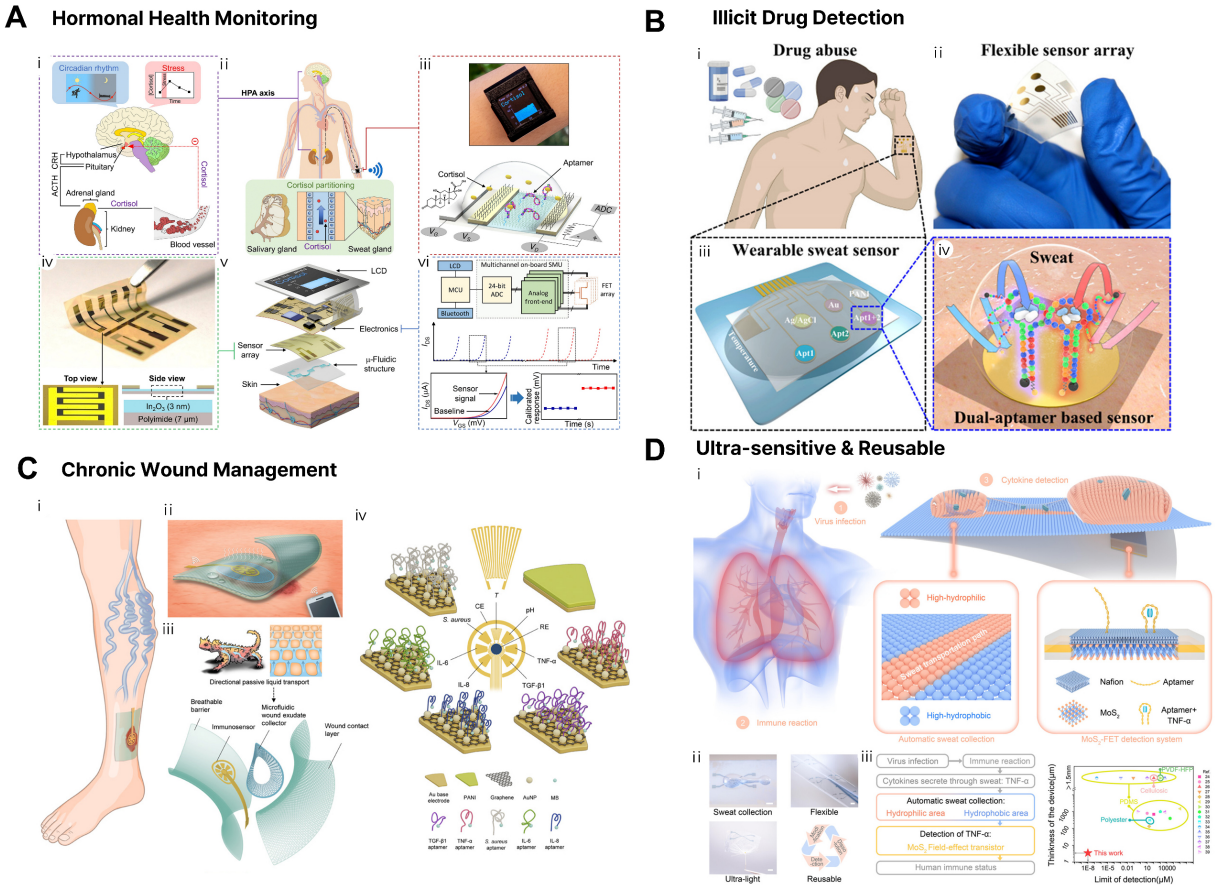

Figure 6. Diverse applications of wearable E-AB sensors for non-invasive sweat analysis. (A) Hormonal health monitoring. Reprinted with permission[141]. Copyright 2022, American Association for the Advancement of Science; (B) Illicit drug detection. Reprinted with permission[142]. Copyright 2022, American Chemical Society; (C) Chronic wound management. Reprinted with permission[146]. Copyright 2021, American Association for the Advancement of Science; (D) Ultra-sensitive & reusable. Reprinted with permission[147]. Copyright 2024, American Chemical Society. ACTH: adrenocorticotropic hormone; CRH: corticotropin-releasing hormone; LCD: liquid crystal display; IL-6: Interleukin-6; IL-8: Interleukin-8; CE: counter electrode; RE: reference electrode; TNF-α: tumor necrosis factor-α; TGF-β1: transforming growth factor–β1; PANI: polyaniline; MB: methylene blue; E-AB: electrochemical aptamer-based.

undiluted sweat with a range of 0.5-500 pM[145].

The advancement of these wearable electrochemical sensing platforms is expanding the scope of analysis beyond sweat to include other cutaneous biofluids such as wound exudate[146]. Recently, a flexible multiplexed immunosensor for point-of-care applications was developed, presenting new possibilities for chronic wound management. This system utilizes microfluidic channels to collect exudate from the wound site and simultaneously monitors inflammatory cytokines [TNF-α, Interleukin-6 (IL-6), IL-1β] alongside physicochemical parameters critical for wound healing (uric acid, pH, and temperature) in real-time [Figure 6C]. This innovation serves as a significant example demonstrating that wearable sensor technology can transcend simple health monitoring to precisely diagnose and manage pathological conditions in localized areas, even within complex biofluid environments.

Furthermore, a study utilizing Nafion and Molybdenum Disulfide (MoS2) FETs incorporated a stepwise wettability structure to enable automatic sweat collection and impurity blocking[147] [Figure 6D]. This system achieved ultra-high sensitivity (down to 10 fM) and, notably, was designed for reusability, highlighting it as a significant alternative to overcome the economic and environmental limitations of disposable wearable sensors.

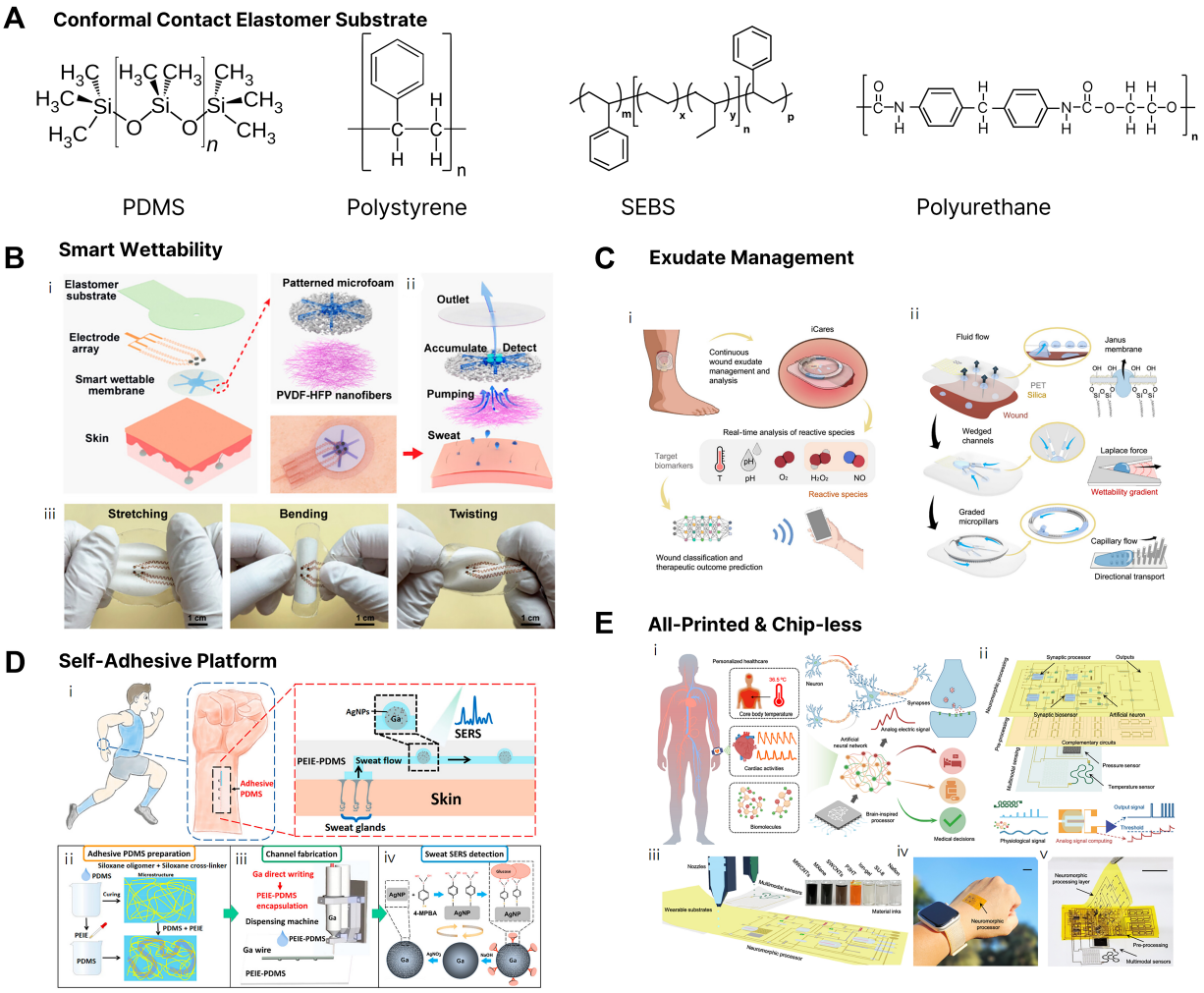

Figure 7. Advanced soft material strategies for conformal skin adhesion and stable bio-interfaces. (A) Conformal contact elastomer substrate. PDMS and polystyrene structures were obtained from Wikimedia Commons (Public Domain); (B) Smart wettability. Reprinted with permission[153]. Copyright 2024, American Chemical Society; (C) Exudate management. Reprinted with permission[135]. Copyright 2025, American Association for the Advancement of Science; (D) Self-adhesive platform. Reprinted with permission[156]. Copyright 2024, American Chemical Society; (E) All-printed & chip-less. Reprinted with permission[157]. Copyright 2025, Springer Nature. PDMS: Polydimethylsiloxane; SEBS: styrene-ethylene-butylene-styrene; PVDF-HFP: poly(vinylidene fluoride-hexafluoropropylene); PET: polyethylene terephthalate; PEIE: polyethylenimine; NP: nanoparticle; SWCNT: single-walled carbon nanotube; MWCNT: mutil-walled carbon nanotube.

Soft materials for skin adhesion of sensor

To ensure the collection of precise and reliable biosignals via wearable sensors, it is essential to minimize mechanical mismatch and maintain conformal contact by accommodating the dynamic curvature and deformation of the skin[148]. Considering that substrate materials and biorecognition layers must possess biocompatibility and non-reactivity in direct contact with the skin, various flexible and stretchable sweat biosensors have been developed using elastomers such as polydimethylsiloxane (PDMS), polystyrene (PS), styrene-ethylene-butylene-styrene (SEBS), polyurethane (PU), and other silicone-based polymers[148,149] [Figure 7A].

Breathability is another critical factor in establishing a stable skin-sensor interface. In this regard, recently developed phase-separated porous nanocomposites offer excellent breathability and ultra-flexibility while maintaining a low percolation threshold. These materials are gaining attention as key components for wireless bioelectronic devices, as they prevent skin inflammation and adhesion loss caused by sweat

accumulation during long-term wear[150].

However, sweat secreted in real-world scenarios acts as a primary factor in weakening adhesion and increasing interfacial impedance[151]. Therefore, functional soft material technologies capable of actively managing fluids like sweat, beyond mere physical flexibility, are required[149]. As a solution, bio-inspired open microfluidic systems with superwetting properties have been proposed. These systems induce spontaneous sweat transport, thereby preventing sensor surface contamination and creating a stable adhesion environment[152]. Furthermore, stretchable and smart wettable sensing patch technologies ensure the accuracy of multiplexed *in situ* analysis by effectively guiding fluid flow even under skin stretching[153] [Figure 7B], while flexible superwettable band platforms enhance sensor utility by simultaneously performing efficient sweat collection and sensing[154]. Expanding the scope of biofluid management, a recent study introduced a microfluidic wearable device specifically designed for the complex environment of human chronic wounds[135]. This system utilizes a soft, biocompatible interface to effectively manage wound exudate - a fluid significantly more viscous and biologically complex than sweat [Figure 7C]. By continuously removing excess exudate, the device not only prevents skin maceration and sensor detachment but also enables the real-time *in situ* analysis of inflammatory biomarkers, demonstrating that advanced fluid-handling soft materials are essential for maintaining stable bio-interfaces on compromised skin.

Material innovations aimed at enhancing adhesion strength itself are also actively progressing. Adhesive biocomposite electrodes capable of maintaining robust attachment even on sweaty skin have enabled long-term continuous electrophysiological monitoring[155]. Additionally, self-adhesive and biocompatible microfluidic platforms utilizing liquid metal to form erasable hotspots have successfully detected glucose in sweat by stably adhering to the skin without additional adhesives[156] [Figure 7D]. Pushing the boundaries of soft material integration, an all-printed, chip-less wearable neuromorphic system has recently been developed[157] [Figure 7E]. This approach eliminates the need for rigid silicon chips by utilizing functional material inks to print both the sensors and the computing elements directly onto flexible substrates. This system achieves efficient multimodal physicochemical monitoring (analyzing both sweat biomarkers and physical signals) while maintaining a seamless, soft interface with the skin, demonstrating that soft materials can now support complex on-sensor data processing.

Moreover, graphene-hydrogel interfaces combine high conductivity with tissue similarity, significantly improving mechanical and electrical coupling in both wearable and implantable devices[158]. When combined with active sweat induction systems such as iontophoresis, these high-performance adhesive materials serve as a crucial foundation for enabling continuous analyte analysis even at rest[159]. In conclusion, soft material technologies for next-generation wearable sensors are evolving to establish stable bio-interfaces in dynamic skin environments by integrally implementing breathability, wettability control, and bio-friendly adhesion beyond simply securing mechanical flexibility.

CHALLENGES AND PERSPECTIVES

To quantitatively contextualize both the progress made and the performance gaps that remain, Table 2 summarizes key analytical parameters of representative E-AB sensors reported across the three target biofluids, alongside the dominant technical hurdles specific to each matrix. This comparative overview reveals that, despite advances in electrode nano-structuring and soft-material integration, a consistent performance ceiling persists, particularly in achieving sub-picomolar sensitivity within undiluted biological matrices and sustaining signal fidelity beyond 72 h of continuous deployment. The following subsections dissect the three most critical challenge domains and propose experimentally grounded pathways toward their resolution.

Table 2. Performance comparison of representative E-AB sensors across blood, ISF, and sweat, highlighting key analytical parameters and dominant technical challenges specific to each biological matrix

Biofluid	Platform or form factor	Target analyte	Limit of detection	Operational stability (in biofluid)	Response time	Dominant technical challenges	Ref.
Blood	Wire electrode (SAM modification)	Vancomycin	Not specified	> 7 days in undiluted serum at 37 °C	Seconds	SAM oxidative degradation; redox-driven thiol desorption accelerated at body temperature	[78]
Blood	Wire electrode (NPG + PEG hydrogel coating)	Kanamycin	μM ~ mM	~ 1 month (*in vitro* serum); ~1 week (*in-vivo*, free-moving rats)	Seconds	Biofouling-induced baseline drift	[132]
Blood	Wire electrode (NPG)	Daunorubicin	100 nM	Multi-hour (*in-vivo*, rat models)	Seconds	Inter-individual pharmacokinetic variability; *In-vivo* baseline signal drift in complex biofluids	[201]
Blood	Implantable microelectrode array (NPG, flexible)	Doxorubicin (intratumoral)	μM level	Hours (*in-vivo*, tumor implantation)	Seconds	Tumor microenvironment heterogeneity; mechanical stress during tissue insertion	[105]
ISF	3D-printed microneedle array (E-AB)	Tobramycin / Vancomycin	μM level	60 min (*in-vivo*, rat)	Sub-second	*In-vivo* environmental noise (precluding high-frequency KDM drift correction); progressive sensor degradation in ISF	[117]
ISF	Acupuncture needle (AuNP-deposited)	Tobramycin / Vancomycin	μM level	Hours (*in-vivo*, continuous)	Sub-second	Needle-to-skin contact stability; ISF–plasma lag time	[95]
ISF	Hydrogel microneedle (MeHA, Wearable Aptalyzer)	Glucose / Lactate	mM level	3 days (*in-vivo*, rat skin)	20 min	Signal lag time due to target diffusion through the hydrogel and slow aptamer dissociation kinetics	[96]
ISF	Solid microneedle patch (human clinical trial)	Vancomycin	nM level	12–24 h in human dermal ISF (primarily 12 h reliable)	5 min	Sensor degradation beyond 12 h; ISF–plasma pharmacokinetic equilibration delay	[202]
Sweat	Skin patch (AuNP-MXene electrode, strand-displacement)	Estradiol	0.14 pM	Hours (on-body, iontophoresis-induced)	~10 min (field-assisted)	Sub-pM target concentration in sweat; ionic strength / pH variability requiring multivariate calibration	[97]
Sweat	Smartwatch (flexible FET array)	Cortisol	pM level	Hours (on-body, continuous)	seconds	Detection of Ultralow Concentration Biomarkers; Debye screening in high ionic strength matrices	[141]
Sweat	Wearable PET patch	TNF-α	0.31 pM	Up to 15 days	Not specified	Trace-level biomarker detection limit; Deformation-induced electrical instability	[145]

E-AB: Electrochemical aptamer-based; ISF: interstitial fluid; SAM: self-assembled monolayer; NPG: Nanoporous Gold; PEG: polyethylene glycol; NP: nanoparticle; FET: Field-Effect Transistors; PET: TNF-α: tumor necrosis factor-α.

Simultaneous achievement of ultra-sensitivity and specificity

First is the simultaneous achievement of ultra-sensitivity and specificity. Macromolecules such as proteins and nucleic acids in whole blood exist in trace amounts (sub-picomolar), demanding much higher sensitivity than metabolite analysis in the millimolar range. While nanostructured electrodes and various signal amplification strategies are being explored, the paradox of increased surface area leading to non-specific

adsorption and reduced signal-to-noise (S/N) ratio must be resolved[160]. Furthermore, to exclude the influence of interferents within the complex matrix of real samples, anti-fouling performance verification in clinically relevant sample environments, rather than simple buffer solutions, must be prioritized. At a more fundamental level, sensitivity in E-AB sensors is intrinsically bounded by the equilibrium dissociation constant (K_D) of the aptamer-target interaction. As established by the population-shift thermodynamic framework, the signal gain of a structure-switching sensor is strictly coupled to its switching equilibrium constant, meaning that sensitivity and dynamic range cannot be simultaneously optimized[94]. This thermodynamic ceiling is further compounded in complex biological matrices, where competitive adsorption from high-abundance proteins such as albumin (~ 40 mg/mL in blood) compresses the available signal window. Electrode geometry improvements alone cannot resolve these constraints. Instead, orthogonal strategies must be co-engineered at the molecular and transduction levels, each tailored to the physicochemical demands of the target biofluid.

Three experimentally validated pathways are proposed here, each matched to a specific biological matrix.

(i) Blood: Aptamer structural engineering. For implantable blood sensors, pseudoknot-assisted two-state aptamer designs constrain the aptamer to only two discrete conformational states, eliminating partially folded intermediates that generate background noise. This approach improves effective sensitivity by nearly an order of magnitude without modifying the electrode or measurement protocol, which is a critical advantage given that the SAM of implantable wire sensors undergoes progressive thiol desorption during multi-day vascular deployment[78,161].

(ii) ISF: Probe density optimization. For microneedle ISF sensors, limited fluid volume and slow analyte diffusion across the dermis create a mass-transport bottleneck. Controlling aptamer surface density over an order-of-magnitude range modulates signal gain from 60% to 200%, with peak performance at the lowest densities where steric crowding is minimized[27]. This principle has guided the adoption of dendritic gold nanoparticle-decorated microneedle tips, which expand aptamer-accessible surface area without enlarging the electrode footprint[95,96].

(iii) Sweat: Electric field-assisted binding. For wearable sweat sensors, target hormones and cytokines often fall below the intrinsic K_D ceiling under passive diffusion conditions, and sweat ionic strength variability continuously perturbs aptamer folding thermodynamics. Applying a controlled electric potential during measurement electrokinetically concentrates charged target molecules at the electrode surface, locally exceeding the bulk concentration and driving occupancy beyond the thermodynamic equilibrium limit without any added reagent. This has been validated in human sweat estradiol sensing (LOD = 0.14 pM), with field-assisted operation reducing incubation time by more than half while preserving full sensor reversibility[97].

Across all three strategies, it is essential that sensitivity gains be validated in the target biological matrix rather than buffer alone. Improvements demonstrated in phosphate-buffered saline have repeatedly failed to translate to undiluted whole blood, ISF, or real human sweat, highlighting that the matrix is itself an inseparable component of the sensing problem[162].

Establishment of calibration-free technologies

Second is the establishment of calibration-free technologies. E-AB sensors often suffer from low reproducibility between sensors due to minute variations in electrode surface or probe density, necessitating cumbersome calibration processes prior to use[109,163-170]. This can be a critical drawback, particularly for continuous monitoring or implantable sensors. As a solution, novel signal mechanisms such as ratiometric

approaches or dual-frequency measurements are being introduced[171-176]. These methods are emerging as promising alternatives to enable calibration-free measurements by canceling out sensor-to-sensor variations. To rigorously contextualize these calibration-free claims, it is critical to examine the specific mechanisms driving this correction, establish standardized performance metrics, and identify the unresolved physical limitations.

(i) Mechanism of drift reduction and variability cancellation. Baseline drift in E-AB sensors primarily arises from two distinct physicochemical processes occurring at the electrode surface: biofouling (nonspecific protein and cellular adsorption that blocks aptamer access, causing a rapid, exponential loss in absolute peak current over the first ~ 1-2 h *in-vivo* or in whole blood) and thiol desorption (electrochemically driven desorption from the gold SAM, producing a slower, approximately linear signal decline thereafter)[177]. Critically, both processes reduce the absolute amplitude of the electrochemical signal at all square-wave voltammetry (SWV) frequencies in a nearly proportional manner, as they simply reduce the total number of accessible methylene blue reporters.

Kinetic Differential Measurements (KDM) and ratiometric approaches exploit this symmetry. By taking the difference or ratio of normalized signals collected at two frequencies (one where target binding increases current and one where it decreases current), the drift term, which scales equally at both frequencies, cancels subtractively. The target-specific signal, however, responds differentially because it reflects a binding-induced change in aptamer electron transfer kinetics, not merely total current amplitude. Similarly, sensor-to-sensor fabrication variability, which manifests as differences in absolute baseline current due to variations in probe density or electrode surface area, also scales with absolute amplitude and is therefore canceled by the ratio operation, rendering the output unitless and independent of fabrication-batch variation[178].

(ii) Practical performance metrics. To standardize the reporting and benchmarking of these calibration-free platforms, specific quantitative metrics should be adopted. For drift, the raw signal loss should be expressed as the percentage of signal loss per hour under relevant deployment conditions (e.g., 37 °C undiluted whole blood or *in-vivo*). For context, when implanted in the jugular veins of anesthetized rats for continuous tobramycin monitoring with one scan every 10 s, conventional DNA-based SAM sensors lose approximately 48% of their baseline signal over 5 h. In contrast, 2′-O-methyl RNA (OMe RNA) aptamer analogs under identical conditions lose only ~ 7% over the same period, a 7-fold improvement[93]. For between-sensor variability, the coefficient of variation (CV) of the normalized output should be reported across ≥ 3 independently fabricated batches. Dual-frequency approaches have shown clinically relevant accuracy even with sensors fabricated without tight surface density control[178]. Finally, the recalibration interval should target ≥ 24 h without recalibration, a critical benchmark considering commercial continuous glucose monitors still require multiple daily recalibrations to maintain ±20% accuracy[172].

(iii) Remaining failure modes. Despite the effectiveness of dual-frequency correction, three fundamental failure modes remain unresolved. Progressive biofouling beyond what KDM can correct: severe or heterogeneous fouling can eventually alter the ratio of the two frequency responses themselves (e.g., by sterically blocking aptamer conformational switching differentially at different timescales), thereby corrupting the correction[177]. This explains why operational lifetimes *in-vivo* remain limited to hours rather than days. Furthermore, motion artifacts: mechanical deformation of the electrode-SAM interface during body movement or blood pulsation can transiently alter the electron transfer rate independently of target binding, generating spurious signals that KDM cannot distinguish from genuine target responses. And temperature dependence: the electron transfer kinetics of the methylene blue reporter shift with temperature, meaning a correction optimized at 37 °C may be inaccurate at body sites with lower or fluctuating

temperatures. Real-time temperature compensation via co-integrated thermal sensors has been shown to reduce quantification error by up to 10% and is recommended as a mitigation strategy[179].

Multiplexing and AI-assisted intelligentization

Third is multiplexing and intelligentization. Accurate disease diagnosis often requires the simultaneous detection of complementary sets of biomarkers rather than a single marker[180,181]. This necessitates integration with microfluidic technologies or high-density array designs. Moreover, the convergence with artificial intelligence (AI) and machine learning (ML) algorithms holds the potential to dramatically enhance the accuracy of personalized diagnostics by denoising complex electrochemical signals and extracting meaningful patterns[182,183]. For multiplexed sensing, a practical near-term pathway is spatially encoded aptamer arrays on flexible substrates, where each electrode zone is independently functionalized for a different target and individually addressable via SWV frequency-based interrogation. This approach eliminates cross-talk between channels without increasing device footprint, which is already demonstrated in wearable E-AB platforms for simultaneous detection of multiple antibiotics in ISF[117] and multiple drugs in sweat[142].

For AI integration, the most critical, and currently underappreciated, prerequisite is the construction of longitudinal *in-vivo* datasets with paired ground-truth reference measurements. Without such structured training data, machine learning models are likely to overfit to bench-scale measurement artifacts rather than learn genuine physiological dynamics. To address the privacy concerns that inevitably accompany the collection of large-scale patient biosensor data, federated learning offers a principled solution: models are trained locally on each patient's device, and only model parameters, not raw signals, are aggregated centrally, preserving patient confidentiality while enabling collaborative learning at scale[184].

CONCLUSION AND OUTLOOK

This review systematically examined E-AB sensor technology for continuous, real-time biomarker monitoring across the blood, ISF, and sweat physiological continuum, with a central focus on soft material strategies that resolve the mechanical and chemical mismatches at the sensor-body interface. As systematically compared in Table 3, the distinct biological constraints imposed by each biofluid underscore why conventional sensing paradigms, including enzymatic sensors and antibody-based immunosensors, fall short as platforms for continuous physiological monitoring, and why the binding-induced conformational change mechanism of E-AB sensors represents a uniquely enabling foundation. To address these biological hurdles, implantable sensors have overcome signal attenuation through nanoporous gold electrode architectures and anti-fouling soft material coatings, enabling real-time intravascular drug monitoring and continuous ISF analysis via microneedle integration, while wearable platforms have expanded non-invasive detection of hormones, drugs, and disease biomarkers through active fluid control technologies including Janus membranes and iontophoresis. Realizing the full clinical potential of this platform will ultimately require the co-engineering of aptamer structural design, calibration-free dual-frequency signal processing, and AI-assisted multiplexed interpretation within a unified, biofluid-aware framework, which is a convergence that positions E-AB sensors as a foundational technology for next-generation personalized precision medicine.

Table 3. Comparison of key sensing technologies for continuous biomonitoring

Criteria	Enzymatic sensors	Antibody-based immunosensors	E-AB sensors
Sensing mechanism	Catalytic oxidation or reduction[162,203]	Affinity binding (irreversible)[185,203]	Binding-induced conformational change[117,162]
Target universality	Narrow (redox-active substrates only)[162]	Broad (protein, small molecules)[203]	Broad (ions, small molecules, proteins, drugs)[117,162]
Reagent-free	X (mediator or cofactor required)[162]	X (labeled secondary Ab often needed)[203]	O[117,162]
Regenerability	Limited (substrate consumed)[162]	Poor (irreversible binding)[185,203]	Excellent (reversible binding)[117,162]
Continuous monitoring	Until enzyme depletion[117,162]	X[203]	O[117,141,162]
Calibration-free potential	X[162]	X[203]	O (signal-on, E-AB ratiometric)[162,178,179]
Chemical modification flexibility	Low (limited enzyme engineering[162]	Low (Ab production constraints)[162,203]	High (SELEX, chemical modification)[117,162]

E-AB: Electrochemical aptamer-based.

DECLARATIONS

Authors' contributions

Literature review, Manuscript conceptualization, Writing - original draft: Lee, H. B.
Supervision, writing - review & editing, project administration: Lee, D.; Ko, S. H.

Availability of data and materials

Not applicable.

AI and AI-assisted tools statement

During the preparation of this manuscript, the AI tool Google Gemini (version 3.0, released 2025-11-19) was used solely for language editing. The tool did not influence the study design, data collection, analysis, interpretation, or the scientific content of the work. All authors take full responsibility for the accuracy, integrity, and final content of the manuscript.

Financial support and sponsorship

This work was supported by National Research Foundation of Korea (grant number RS-2025-11092968, RS-2023-00216821, RS-2022-NR068144).

Conflicts of interest

Ko, S. H. is an Editorial Board Member of the journal *Soft Science* but is not involved in any steps of editorial processing, notably including reviewer selection, manuscript handling, or decision-making. The other authors declare that there are no conflicts of interest.

Ethical approval and consent to participate

Not applicable.

Consent for publication

Not applicable.

REFERENCES

1. Suami, H.; Scaglioni, M. Anatomy of the lymphatic system and the lymphosome concept with reference to lymphedema. *Semin. Plast. Surg.* **2018**, *32*, 005-11. DOI PubMed PMC
2. Ono, S.; Egawa, G.; Kabashima, K. Regulation of blood vascular permeability in the skin. *Inflamm. Regener.* **2017**, *37*, 11. DOI PubMed PMC

3. Vermeer, B. J.; Reman, F. C.; Van Gent, C. M. The determination of lipids and proteins in suction blister fluid. *J. Investig. Dermatol.* **1979**, *73*, 303-5. DOI
4. Broza, Y. Y.; Zhou, X.; Yuan, M.; et al. Disease detection with molecular biomarkers: from chemistry of body fluids to nature-inspired chemical sensors. *Chem. Rev.* **2019**, *119*, 11761-817. DOI
5. Crowley, E.; Di Nicolantonio, F.; Loupakis, F.; Bardelli, A. Liquid biopsy: monitoring cancer-genetics in the blood. *Nat. Rev. Clin. Oncol.* **2013**, *10*, 472-84. DOI
6. Alix-panabières, C.; Pantel, K. Clinical applications of circulating tumor cells and circulating tumor DNA as liquid biopsy. *Cancer. Discovery.* **2016**, *6*, 479-91. DOI
7. Sturgeon, C. M.; Duffy, M. J.; Stenman, U.; et al. National academy of clinical biochemistry laboratory medicine practice guidelines for use of tumor markers in testicular, prostate, colorectal, breast, and ovarian cancers. *Clin. Chem.* **2008**, *54*, e11-79. DOI
8. Ludwig, J. A.; Weinstein, J. N. Biomarkers in cancer staging, prognosis and treatment selection. *Nat. Rev. Cancer.* **2005**, *5*, 845-56. DOI
9. Su, J.; Chen, S.; Dou, Y.; et al. Smartphone-based electrochemical biosensors for directly detecting serum-derived exosomes and monitoring their secretion. *Anal. Chem.* **2022**, *94*, 3235-44. DOI
10. Wu, A. H.; Apple, F. S.; Gibler, W. B.; Jesse, R. L.; Warshaw, M. M.; Valdes, R. National academy of clinical biochemistry standards of laboratory practice: recommendations for the use of cardiac markers in coronary artery diseases. *Clin. Chem.* **1999**, *45*, 1104-21. DOI
11. Mahato, K.; Wang, J. Electrochemical sensors: from the bench to the skin. *Sensor. Actuat. B-Chem.* **2021**, *344*, 130178. DOI
12. Zhou, J. Z.; Kane, S.; Ramsey, C.; et al. Comparison of early- and late-stage breast and colorectal cancer diagnoses during vs before the COVID-19 pandemic. *JAMA. Netw. Open.* **2022**, *5*, e2148581. DOI PubMed PMC
13. Renard, E. Implantable continuous glucose sensors. *Curr. Diabetes. Rev.* **2008**, *4*, 169-74. DOI
14. Ward, W. K.; House, J. L.; Birck, J.; Anderson, E. M.; Jansen, L. B. A wire-based dual-analyte sensor for glucose and lactate: *in vitro* and *in vivo* evaluation. *Diabetes. Technol. The.* **2004**, *6*, 389-401. DOI
15. Chergui, K.; Suaud-Chagny, M.; Gonon, F. Nonlinear relationship between impulse flow, dopamine release and dopamine elimination in the rat brain *in vivo*. *Neuroscience* **1994**, *62*, 641-5. DOI
16. Kraft, J.; Osterhaus, G.; Ortiz, A.; Garris, P.; Johnson, M. In vivo dopamine release and uptake impairments in rats treated with 3-nitropropionic acid. *Neuroscience* **2009**, *161*, 940-9. DOI
17. Zhang, J.; Jaquins-Gerstl, A.; Nesbitt, K. M.; Rutan, S. C.; Michael, A. C.; Weber, S. G. *In vivo* monitoring of serotonin in the striatum of freely moving rats with one minute temporal resolution by online microdialysis-capillary high-performance liquid chromatography at elevated temperature and pressure. *Anal. Chem.* **2013**, *85*, 9889-97. DOI
18. Wassum, K. M.; Tolosa, V. M.; Tseng, T. C.; Balleine, B. W.; Monbouquette, H. G.; Maidment, N. T. Transient extracellular glutamate events in the basolateral amygdala track reward-seeking actions. *J. Neurosci.* **2012**, *32*, 2734-46. DOI
19. Sarter, M.; Kim, Y. Interpreting chemical neurotransmission *in vivo*: techniques, time scales, and theories. *ACS. Chem. Neurosci.* **2014**, *6*, 8-10. DOI
20. Gaster, R. S.; Hall, D. A.; Nielsen, C. H.; et al. Matrix-insensitive protein assays push the limits of biosensors in medicine. *Nat. Med.* **2009**, *15*, 1327-32. DOI PubMed PMC
21. Plaxco, K. W.; Soh, H. T. Switch-based biosensors: a new approach towards real-time, *in vivo* molecular detection. *Trends. Biotechnol.* **2011**, *29*, 1-5. DOI PubMed PMC
22. Couture, M.; Zhao, S. S.; Masson, J. Modern surface plasmon resonance for bioanalytics and biophysics. *Phys. Chem. Chem. Phys.* **2013**, *15*, 11190-216. DOI
23. Marsh, Z. M.; Lantz, K. A.; Stefik, M. QCM detection of molecule-nanoparticle interactions for ligand shells of varying morphology. *Nanoscale* **2018**, *10*, 19107-16. DOI
24. Vaisocherová, H.; Brynda, E.; Homola, J. Functionalizable low-fouling coatings for label-free biosensing in complex biological media: advances and applications. *Anal. Bioanal. Chem.* **2015**, *407*, 3927-53. DOI
25. Breault-turcot, J.; Masson, J. Microdialysis SPR: diffusion-gated sensing in blood. *Chem. Sci.* **2015**, *6*, 4247-54. DOI PubMed PMC
26. Arroyo-currás, N.; Somerson, J.; Vieira, P. A.; Ploense, K. L.; Kippin, T. E.; Plaxco, K. W. Real-time measurement of small molecules directly in awake, ambulatory animals. *Proc. Natl. Acad. Sci. U.S.A.* **2017**, *114*, 645-50. DOI PubMed PMC
27. White, R. J.; Phares, N.; Lubin, A. A.; Xiao, Y.; Plaxco, K. W. Optimization of electrochemical aptamer-based sensors via optimization of probe packing density and surface chemistry. *Langmuir* **2008**, *24*, 10513-8. DOI PubMed PMC
28. Dauphin-ducharme, P.; Yang, K.; Arroyo-currás, N.; et al. Electrochemical aptamer-based sensors for improved therapeutic drug monitoring and high-precision, feedback-controlled drug delivery. *ACS. Sens.* **2019**, *4*, 2832-7. DOI PubMed PMC
29. Idili, A.; Arroyo-currás, N.; Ploense, K. L.; et al. Seconds-resolved pharmacokinetic measurements of the chemotherapeutic irinotecan *in situ* in the living body. *Chem. Sci.* **2019**, *10*, 8164-70. DOI
30. Swensen, J. S.; Xiao, Y.; Ferguson, B. S.; et al. Continuous, real-time monitoring of cocaine in undiluted blood serum via a microfluidic, electrochemical aptamer-based sensor. *J. Am. Chem. Soc.* **2009**, *131*, 4262-6. DOI PubMed PMC

31. Parolo, C.; Idili, A.; Ortega, G.; et al. Real-time monitoring of a protein biomarker. *ACS. Sens.* **2020**, *5*, 1877-81. DOI PubMed PMC
32. Liu, Y.; Kwa, T.; Revzin, A. Simultaneous detection of cell-secreted TNF-α and IFN-γ using micropatterned aptamer-modified electrodes. *Biomaterials* **2012**, *33*, 7347-55. DOI PubMed PMC
33. Mayer, M. D.; Lai, R. Y. Effects of redox label location on the performance of an electrochemical aptamer-based tumor necrosis factor-alpha sensor. *Talanta* **2018**, *189*, 585-91. DOI
34. Idili, A.; Gerson, J.; Parolo, C.; Kippin, T.; Plaxco, K. W. An electrochemical aptamer-based sensor for the rapid and convenient measurement of l-tryptophan. *Anal. Bioanal. Chem.* **2019**, *411*, 4629-35. DOI PubMed PMC
35. Idili, A.; Parolo, C.; Ortega, G.; Plaxco, K. W. Calibration-free measurement of phenylalanine levels in the blood using an electrochemical aptamer-based sensor suitable for point-of-care applications. *ACS. Sens.* **2019**, *4*, 3227-33. DOI PubMed PMC
36. Arroyo-Currás, N.; Dauphin-Ducharme, P.; Ortega, G.; Ploense, K. L.; Kippin, T. E.; Plaxco, K. W. Subsecond-resolved molecular measurements in the living body using chronoamperometrically interrogated aptamer-based sensors. *ACS. Sens.* **2017**, *3*, 360-6. DOI
37. Arroyo-currás, N.; Ortega, G.; Copp, D. A.; et al. High-precision control of plasma drug levels using feedback-controlled dosing. *ACS. Pharmacol. Transl. Sci.* **2018**, *1*, 110-8. DOI PubMed PMC
38. Anitha, K.; Posinasetty, B.; Naveen Kumari, K.; et al. Liquid biopsy for precision diagnostics and therapeutics. *Clin. Chim. Acta.* **2024**, *554*, 117746. DOI
39. Zhou, Y.; Tao, L.; Qiu, J.; et al. Tumor biomarkers for diagnosis, prognosis and targeted therapy. *Sig. Transduct. Target. Ther.* **2024**, *9*, 132. DOI PubMed PMC
40. Yu, M.; Tyson, C.; Limburg, P. J.; Beer, T. M. A flexible quantitative framework to assess the potential contribution of early cancer detection to improved cancer survival. *J. Clin. Oncol.* **2023**, *41*, e22508. DOI
41. Childs, A.; Mayol, B.; Lasalde-Ramírez, J. A.; Song, Y.; Sempionatto, J. R.; Gao, W. Diving into sweat: advances, challenges, and future directions in wearable sweat sensing. *ACS. Nano.* **2024**, *18*, 24605-16. DOI PubMed PMC
42. Davis, N.; Heikenfeld, J.; Milla, C.; Javey, A. The challenges and promise of sweat sensing. *Nat. Biotechnol.* **2024**, *42*, 860-71. DOI
43. Heikenfeld, J.; Jajack, A.; Feldman, B.; et al. Accessing analytes in biofluids for peripheral biochemical monitoring. *Nat. Biotechnol.* **2019**, *37*, 407-19. DOI
44. Tran, B. Q.; Miller, P. R.; Taylor, R. M.; et al. Proteomic characterization of dermal interstitial fluid extracted using a novel microneedle-assisted technique. *J. Proteome. Res.* **2017**, *17*, 479-85. DOI
45. Taylor, R. M.; Miller, P. R.; Ebrahimi, P.; Polsky, R.; Baca, J. T. Minimally-invasive, microneedle-array extraction of interstitial fluid for comprehensive biomedical applications: transcriptomics, proteomics, metabolomics, exosome research, and biomarker identification. *Lab. Anim.* **2018**, *52*, 526-30. DOI
46. Miller, P. R.; Taylor, R. M.; Tran, B. Q.; et al. Extraction and biomolecular analysis of dermal interstitial fluid collected with hollow microneedles. *Commun. Biol.* **2018**, *1*, 173. DOI PubMed PMC
47. Davis, M. J.; Rahbar, E.; Gashev, A. A.; Zawieja, D. C.; Moore, J. E. Determinants of valve gating in collecting lymphatic vessels from rat mesentery. *Am. J. Physiol.-Heart. C.* **2011**, *301*, H48-60. DOI PubMed PMC
48. Mendoza, E.; Schmid-Scho¨nbein, G. W. A model for mechanics of primary lymphatic valves. *J. Biomech. Eng.* **2003**, *125*, 407-14. DOI
49. Bendayan, M. Morphological and cytochemical aspects of capillary permeability. *Microsc. Res. Tech.* **2002**, *57*, 327-49. DOI
50. Vink, H.; Duling, B. R. Capillary endothelial surface layer selectively reduces plasma solute distribution volume. *Am. J. Physiol.-Heart. C.* **2000**, *278*, H285-9. DOI
51. Michel, C. C.; Curry, F. E. Microvascular permeability. *Physiol. Rev.* **1999**, *79*, 703-61. DOI
52. Tuma, P. L.; Hubbard, A. L. Transcytosis: crossing cellular barriers. *Physiol. Rev.* **2003**, *83*, 871-932. DOI
53. Geyer, P. E.; Holdt, L. M.; Teupser, D.; Mann, M. Revisiting biomarker discovery by plasma proteomics. *Mol. Syst. Biol.* **2017**, *13*, MSB156297. DOI
54. Kasemo, B.; Gold, J. Implant surfaces and interface processes. *Adv. Dent. Res.* **1999**, *13*, 8-20. DOI
55. Zhang, Z.; Zhang, M.; Chen, S.; Horbett, T. A.; Ratner, B. D.; Jiang, S. Blood compatibility of surfaces with superlow protein adsorption. *Biomaterials* **2008**, *29*, 4285-91. DOI
56. Anderson, N. L.; Anderson, N. G. The human plasma proteome. *Mol. Cell. Proteomics.* **2002**, *1*, 845-67. DOI
57. Anderson, J. M. Biological responses to materials. *Annu. Rev. Mater. Res.* **2001**, *31*, 81-110. DOI
58. Hower, J. C.; Bernards, M. T.; Chen, S.; Tsao, H.; Sheng, Y.; Jiang, S. Hydration of "nonfouling" functional groups. *J. Phys. Chem. B.* **2008**, *113*, 197-201. DOI
59. Lavery, K. S.; Rhodes, C.; Mcgraw, A.; Eppihimer, M. J. Anti-thrombotic technologies for medical devices. *Adv. Drug. Delivery. Rev.* **2017**, *112*, 2-11. DOI
60. Jaffer, I. H.; Weitz, J. I. The blood compatibility challenge. Part 1: blood-contacting medical devices: the scope of the problem. *Acta. Biomater.* **2019**, *94*, 2-10. DOI

61. Wallace, A.; Albadawi, H.; Patel, N.; et al. Anti-fouling strategies for central venous catheters. *Cardiovasc. Diagn. Ther.* **2017**, *7*. Suppl, S246-57. DOI PubMed PMC
62. Wilson, C. J.; Clegg, R. E.; Leavesley, D. I.; Pearcy, M. J. Mediation of biomaterial-cell interactions by adsorbed proteins: a review. *Tissue. Eng.* **2005**, *11*, 1-18. DOI
63. Singha, P.; Locklin, J.; Handa, H. A review of the recent advances in antimicrobial coatings for urinary catheters. *Acta. Biomater.* **2017**, *50*, 20-40. DOI PubMed PMC
64. Gupta, P.; Sarkar, S.; Das, B.; Bhattacharjee, S.; Tribedi, P. Biofilm, pathogenesis and prevention - a journey to break the wall: a review. *Arch. Microbiol.* **2015**, *198*, 1-15. DOI
65. Plachouras, D.; Lepape, A.; Suetens, C. ECDC definitions and methods for the surveillance of healthcare-associated infections in intensive care units. *Intensive. Care. Med.* **2018**, *44*, 2216-8. DOI PubMed PMC
66. Kostakioti, M.; Hadjifrangiskou, M.; Hultgren, S. J. Bacterial biofilms: development, dispersal, and therapeutic strategies in the dawn of the postantibiotic era. *CSH. Perspect. Med.* **2013**, *3*, a010306. DOI PubMed PMC
67. Kolluru, C.; Williams, M.; Chae, J.; Prausnitz, M. R. Recruitment and collection of dermal interstitial fluid using a microneedle patch. *Adv. Healthc. Mater.* **2019**, *8*, 1801262. DOI PubMed PMC
68. Laszlo, E.; De Crescenzo, G.; Nieto-argüello, A.; Banquy, X.; Brambilla, D. Superswelling microneedle arrays for dermal interstitial fluid (prote)omics. *Adv. Funct. Mater.* **2021**, *31*, 2106061. DOI
69. Himawan, A.; Vora, L. K.; Permana, A. D.; et al. Where microneedle meets biomarkers: futuristic application for diagnosing and monitoring localized external organ diseases. *Adv. Healthc. Mater.* **2022**, *12*, 2202066. DOI PubMed PMC
70. Xu, D.; Guo, D.; Zhang, J.; et al. Innovative tumor interstitial fluid-triggered carbon dot-docetaxel nanoassemblies for targeted drug delivery and imaging of HER2-positive breast cancer. *Int. J. Pharm.* **2024**, *657*, 124145. DOI
71. Jasuja, H.; Jaswandkar, S. V.; Katti, D. R.; Katti, K. S. Interstitial fluid flow contributes to prostate cancer invasion and migration to bone; study conducted using a novel horizontal flow bioreactor. *Biofabrication* **2023**, *15*, 025017. DOI PubMed PMC
72. Acs, M.; Acs, R.; Briandi, C.; Eubanks, E.; Rehman, O.; Zhuang, H. Exploration of the relevance of microRNA signatures for cancer detection and multiclass cancer classification. *IEEE. Access.* **2023**, *11*, 57268-84. DOI
73. Yan, S.; Zheng, H.; Zhao, J.; Gao, M.; Zhang, X. Quantification of GPC1(+) exosomes based on MALDI-TOF MS in situ signal amplification for pancreatic cancer discrimination and evaluation. *Anal. Chem.* **2023**, *95*, 10196-203. DOI
74. Chen, Y.; Gao, D.; Zhu, Q.; et al. Rapid exosome isolation and *in situ* multiplexed detection of exosomal surface proteins and microRNAs on microfluidic platform. *Analyst* **2023**, *148*, 2387-94. DOI
75. Fogh-Andersen, N.; Altura, B. M.; Altura, B. T.; Siggaard-Andersen, O. Composition of interstitial fluid. *Clin. Chem.* **1995**, *41*, 1522-5. DOI
76. Al Sulaiman, D.; Chang, J. Y. H.; Bennett, N. R.; et al. Hydrogel-coated microneedle arrays for minimally invasive sampling and sensing of specific circulating nucleic acids from skin interstitial fluid. *ACS. Nano.* **2019**, *13*, 9620-8. DOI PubMed PMC
77. Li, Y.; Wang, Y.; Mei, R.; et al. Hydrogel-coated SERS microneedles for drug monitoring in dermal interstitial fluid. *ACS. Sens.* **2024**, *9*, 2567-74. DOI
78. Watkins, Z.; Karajic, A.; Young, T.; White, R.; Heikenfeld, J. Week-long operation of electrochemical aptamer sensors: new insights into self-assembled monolayer degradation mechanisms and solutions for stability in serum at body temperature. *ACS. Sens.* **2023**, *8*, 1119-31. DOI PubMed PMC
79. Harder, J.; Schröder, J. RNase 7, a novel innate immune defense antimicrobial protein of healthy human skin. *J. Biol. Chem.* **2002**, *277*, 46779-84. DOI
80. Shukla, S.; Machekposhti, S. A.; Joshi, N.; Joshi, P.; Narayan, R. J. Microneedle-integrated device for transdermal sampling and analyses of targeted biomarkers. *Small. Sci.* **2023**, *3*, 2200087. DOI
81. Facchinetti, A.; Sparacino, G.; Cobelli, C. Reconstruction of glucose in plasma from interstitial fluid continuous glucose monitoring data: role of sensor calibration. *J. Diabetes. Sci. Technol.* **2007**, *1*, 617-23. DOI
82. Shao, J.; Li, X.; Li, Y.; Lin, J.; Huang, P. Self-heating multistage microneedle patch for topical therapy of skin cancer. *Adv. Mater.* **2024**, *36*, 2308217. DOI
83. Sonner, Z.; Wilder, E.; Heikenfeld, J.; et al. The microfluidics of the eccrine sweat gland, including biomarker partitioning, transport, and biosensing implications. *Biomicrofluidics* **2015**, *9*, 031301. DOI PubMed PMC
84. Luchini, A.; Fredolini, C.; Espina, B.; et al. Nanoparticle technology: addressing the fundamental roadblocks to protein biomarker discovery. *Curr. Mol. Med.* **2010**, *10*, 133-41. DOI PubMed PMC
85. Boysen, T. C.; Yanagawa, S.; Sato, F.; Sato, K. A modified anaerobic method of sweat collection. *J. Appl. Physiol.* **1984**, *56*, 1302-7. DOI
86. Jajack, A.; Brothers, M.; Kasting, G.; Heikenfeld, J. Enhancing glucose flux into sweat by increasing paracellular permeability of the sweat gland. *PLoS. ONE.* **2018**, *13*, e0200009. DOI PubMed PMC

87. Crandall, C. G. Mechanisms and controllers of eccrine sweating in humans. *Front. Biosci.* **2010**, *S2*, 685-96. DOI PubMed PMC
88. Hianik, T.; Ostatná, V.; Sonlajtnerova, M.; Grman, I. Influence of ionic strength, pH and aptamer configuration for binding affinity to thrombin. *Bioelectrochemistry* **2007**, *70*, 127-33. DOI
89. Csősz, É.; Emri, G.; Kalló, G.; Tsaprailis, G.; Tőzsér, J. Highly abundant defense proteins in human sweat as revealed by targeted proteomics and label-free quantification mass spectrometry. *J. Eur. Acad. Dermatol. Venereol.* **2015**, *29*, 2024-31. DOI
90. Gao, W.; Emaminejad, S.; Nyein, H. Y. Y.; et al. Fully integrated wearable sensor arrays for multiplexed in situ perspiration analysis. *Nature* **2016**, *529*, 509-14. DOI PubMed PMC
91. Jia, M.; Chew, W. M.; Feinstein, Y.; Skeath, P.; Sternberg, E. M. Quantification of cortisol in human eccrine sweat by liquid chromatography - tandem mass spectrometry. *Analyst* **2016**, *141*, 2053-60. DOI
92. Heikenfeld, J. Non-invasive analyte access and sensing through eccrine sweat: challenges and outlook circa 2016. *Electroanalysis* **2016**, *28*, 1242-9. DOI
93. Leung, K. K.; Gerson, J.; Emmons, N.; Heemstra, J. M.; Kippin, T. E.; Plaxco, K. W. The use of xenonucleic acids significantly reduces the *in vivo* drift of electrochemical aptamer-based sensors. *Angew. Chem. Int. Ed.* **2024**, *63*, e202316678. DOI PubMed PMC
94. Vallée-bélisle, A.; Ricci, F.; Plaxco, K. W. Thermodynamic basis for the optimization of binding-induced biomolecular switches and structure-switching biosensors. *Proc. Natl. Acad. Sci. U.S.A.* **2009**, *106*, 13802-7. DOI PubMed PMC
95. Lin, S.; Cheng, X.; Zhu, J.; et al. Wearable microneedle-based electrochemical aptamer biosensing for precision dosing of drugs with narrow therapeutic windows. *Sci. Adv.* **2022**, *8*, eabq4539. DOI PubMed PMC
96. Bakhshandeh, F.; Zheng, H.; Barra, N. G.; et al. Wearable aptalyzer integrates microneedle and electrochemical sensing for *in vivo* monitoring of glucose and lactate in live animals. *Adv. Mater.* **2024**, *36*, 2313743. DOI
97. Ye, C.; Wang, M.; Min, J.; et al. A wearable aptamer nanobiosensor for non-invasive female hormone monitoring. *Nat. Nanotechnol.* **2023**, *19*, 330-7. DOI PubMed PMC
98. He, R.; Liu, H.; Niu, Y.; Zhang, H.; Genin, G. M.; Xu, F. Flexible miniaturized sensor technologies for long-term physiological monitoring. *npj. Flex. Electron.* **2022**, *6*, 20. DOI
99. Han, S.; Yamamoto, S.; Jung, C.; Jin, D. Y.; Lee, T.; Kim, J. Wearable sensors for monitoring chronic kidney disease. *Commun. Mater.* **2024**, *5*, 153. DOI
100. Timpel, J.; Klinghammer, S.; Riemenschneider, L.; et al. Sensors for *in situ* monitoring of oral and dental health parameters in saliva. *Clin. Oral. Investig.* **2023**, *27*, 5719-36. DOI
101. Pandit, P.; Crewther, B.; Cook, C.; Punyadeera, C.; Pandey, A. K. Sensing methods for stress biomarker detection in human saliva: a new frontier for wearable electronics and biosensing. *Mater. Adv.* **2024**, *5*, 5339-50. DOI
102. Li, X.; Liu, S.; Huang, X.; et al. Aptamers-based wearable electrochemical sensors for continuous monitoring of biomarkers *in vivo*. *Microsyst. Nanoeng.* **2025**, *11*, 241. DOI
103. Holmlin, R. E.; Chen, X.; Chapman, R. G.; Takayama, S.; Whitesides, G. M. Zwitterionic SAMs that resist nonspecific adsorption of protein from aqueous buffer. *Langmuir* **2001**, *17*, 2841-50. DOI
104. Ferguson, B. S.; Hoggarth, D. A.; Maliniak, D.; et al. Real-time, aptamer-based tracking of circulating therapeutic agents in living animals. *Sci. Transl. Med.* **2013**, *5*. DOI PubMed PMC
105. Seo, J.; Fu, K.; Correa, S.; Eisenstein, M.; Appel, E. A.; Soh, H. T. Real-time monitoring of drug pharmacokinetics within tumor tissue in live animals. *Sci. Adv.* **2022**, *8*, eabk2901. DOI PubMed PMC
106. Fu, K.; Seo, J. W.; Kesler, V.; et al. Accelerated electron transfer in nanostructured electrodes improves the sensitivity of electrochemical biosensors. *Adv. Sci.* **2021**, *8*, 2102495. DOI
107. Downs, A. M.; Gerson, J.; Hossain, M. N.; et al. Nanoporous gold for the miniaturization of *in vivo* electrochemical aptamer-based sensors. *ACS. Sens.* **2021**, *6*, 2299-306. DOI
108. Daggumati, P.; Matharu, Z.; Seker, E. Effect of nanoporous gold thin film morphology on electrochemical DNA sensing. *Anal. Chem.* **2015**, *87*, 8149-56. DOI
109. Yang, W.; Gerasimov, J. Y.; Lai, R. Y. Folding-based electrochemical DNA sensor fabricated on a gold-plated screen-printed carbon electrode. *Chem. Commun.* **2009**, 2902. DOI
110. Matharu, Z.; Daggumati, P.; Wang, L.; Dorofeeva, T. S.; Li, Z.; Seker, E. Nanoporous-gold-based electrode morphology libraries for investigating structure-property relationships in nucleic acid based electrochemical biosensors. *ACS. Appl. Mater. Interfaces.* **2017**, *9*, 12959-66. DOI
111. Arroyo-currás, N.; Scida, K.; Ploense, K. L.; Kippin, T. E.; Plaxco, K. W. High surface area electrodes generated via electrochemical roughening improve the signaling of electrochemical aptamer-based biosensors. *Anal. Chem.* **2017**, *89*, 12185-91. DOI
112. Welsh, J. B.; Psavko, S.; Zhang, X.; Gao, P.; Balo, A. K. Comparisons of fifth-, sixth-, and seventh-generation continuous glucose monitoring systems. *J. Diabetes. Sci. Technol.* **2022**, *18*, 143-7. DOI PubMed PMC

113. Battelino, T.; Alexander, C. M.; Amiel, S. A.; et al. Continuous glucose monitoring and metrics for clinical trials: an international consensus statement. *Lancet. Diabetes. Endo.* **2023**, *11*, 42-57. DOI
114. Chmayssem, A.; Nadolska, M.; Tubbs, E.; et al. Insight into continuous glucose monitoring: from medical basics to commercialized devices. *Microchim. Acta.* **2023**, *190*, 177. DOI
115. Downs, A. M.; Bolotsky, A.; Weaver, B. M.; et al. Microneedle electrochemical aptamer-based sensing: real-time small molecule measurements using sensor-embedded, commercially-available stainless steel microneedles. *Biosens. Bioelectron.* **2023**, *236*, 115408. DOI
116. Reynoso, M.; Chang, A.; Wu, Y.; et al. 3D-printed, aptamer-based microneedle sensor arrays using magnetic placement on live rats for pharmacokinetic measurements in interstitial fluid. *Biosens. Bioelectron.* **2024**, *244*, 115802. DOI
117. Wu, Y.; Tehrani, F.; Teymourian, H.; et al. Microneedle aptamer-based sensors for continuous, real-time therapeutic drug monitoring. *Anal. Chem.* **2022**, *94*, 8335-45. DOI PubMed PMC
118. Keyvani, F.; Ghavaminejad, P.; Saleh, M. A.; et al. Integrated electrochemical aptamer biosensing and colorimetric pH monitoring via hydrogel microneedle assays for assessing antibiotic treatment. *Adv. Sci.* **2024**, *11*, 2309027. DOI PubMed PMC
119. Chiang, P.; Lin, X.; Shin, S.; et al. Real-time and continuous L-tryptophan monitoring by electrochemical aptamer-enabled microneedle sensor array. *Sensor. Actuat. B-Chem.* **2026**, *449*, 139056. DOI
120. Yue Jing, L.; Fan, Y.; Zhi Chen, B.; et al. An aptamer-integrated conductive microneedle biosensor for real-time transdermal cortisol monitoring. *Chem. Eng. J.* **2024**, *502*, 157488. DOI
121. Keyvani, F.; Zheng, H.; Kaysir, M. R.; et al. A hydrogel microneedle assay combined with nucleic acid probes for on-site detection of small molecules and proteins. *Angew. Chem. Int. Ed.* **2023**, *62*, e202301624. DOI
122. Yuan, R.; Cai, J.; Li, J.; et al. Integrated microneedle aptasensing platform toward point-of-care monitoring of bacterial infections and treatment. *ACS. Sens.* **2025**, *10*, 5684-93. DOI
123. Fakeih, E.; Shetty, S. S.; Hanif, W.; Mutabagani, K.; Salama, K. N.; Alsulaiman, D. A Microneedle-based Ige aptasensor for transdermal detection of food allergy sensitization. *ACS. Materials. Lett.* **2025**, *7*, 3595-603. DOI
124. Friedel, M.; Werbovetz, B.; Drexelius, A.; et al. Continuous molecular monitoring of human dermal interstitial fluid with microneedle-enabled electrochemical aptamer sensors. *Lab. Chip.* **2023**, *23*, 3289-99. DOI PubMed PMC
125. Chen, S.; Li, L.; Zhao, C.; Zheng, J. Surface hydration: Principles and applications toward low-fouling/nonfouling biomaterials. *Polymer* **2010**, *51*, 5283-93. DOI
126. Kesler, V.; Fu, K.; Chen, Y.; et al. Tailoring electrode surface charge to achieve discrimination and quantification of chemically similar small molecules with electrochemical aptamers. *Adv. Funct. Mater.* **2022**, *33*, 2208534. DOI PubMed PMC
127. Mcgowan, M. P.; Trowbridge, A. J.; Reitemeier, J.; Jordan, K. M.; Fu, K. X. Surface charge effects of monovalent and zwitterionic monolayers to differentiate structurally similar aminoglycosides with electrochemical aptamer biosensors. *Biosens. Bioelectron.* **2025**, *276*, 117229. DOI
128. Li, S.; Wang, Y.; Zhang, Z.; Wang, Y.; Li, H.; Xia, F. Exploring end-group effect of alkanethiol self-assembled monolayers on electrochemical aptamer-based sensors in biological fluids. *Anal. Chem.* **2021**, *93*, 5849-55. DOI
129. Li, H.; Dauphin-Ducharme, P.; Arroyo-Currás, N.; et al. A biomimetic phosphatidylcholine-terminated monolayer greatly improves the *in vivo* performance of electrochemical aptamer-based sensors. *Angew. Chem. Int. Ed.* **2017**, *56*, 7492-5. DOI PubMed PMC
130. Duan, H.; Peng, S.; He, S.; et al. Antifouling zwitterionic coating enhances electrochemical aptamer-based sensors for therapeutic drug monitoring. *Nano. Today.* **2026**, *66*, 102892. DOI
131. Kim, S.; Gim, T.; Jeong, Y.; Ryu, J. H.; Kang, S. M. Facile construction of robust multilayered PEG films on polydopamine-coated solid substrates for marine antifouling applications. *ACS. Appl. Mater. Interfaces.* **2017**, *10*, 7626-31. DOI
132. Chen, Y.; Fu, K. X.; Cotton, R.; et al. A biochemical sensor with continuous extended stability *in vivo*. *Nat. Biomed. Eng.* **2025**, *9*, 1517-30. DOI
133. Li, S.; Dai, J.; Zhu, M.; et al. Implantable hydrogel-protective DNA aptamer-based sensor supports accurate, continuous electrochemical analysis of drugs at multiple sites in living rats. *ACS. Nano.* **2023**, *17*, 18525-38. DOI
134. Huldin, G. F.; Huang, J.; Reitemeier, J.; Fu, K. X. Nafion coated nanopore electrode for improving electrochemical aptamer-based biosensing. *Faraday. Discuss.* **2025**, *257*, 316-32. DOI
135. Wang, C.; Fan, K.; Shirzaei Sani, E.; et al. A microfluidic wearable device for wound exudate management and analysis in human chronic wounds. *Sci. Transl. Med.* **2025**, *17*, eadt0882. DOI PubMed PMC
136. Wang, M.; Ye, C.; Yang, Y.; et al. Printable molecule-selective core-shell nanoparticles for wearable and implantable sensing. *Nat. Mater.* **2025**, *24*, 589-98. DOI
137. Xu, C.; Song, Y.; Sempionatto, J. R.; et al. A physicochemical-sensing electronic skin for stress response monitoring. *Nat. Electron.* **2024**, *7*, 168-79. DOI PubMed PMC

138. Song, Y.; Tay, R. Y.; Li, J.; et al. 3D-printed epifluidic electronic skin for machine learning–powered multimodal health surveillance. *Sci. Adv.* **2023**, *9*, eadi6492. DOI PubMed PMC
139. Min, J.; Demchyshyn, S.; Sempionatto, J. R.; et al. An autonomous wearable biosensor powered by a perovskite solar cell. *Nat. Electron.* **2023**, *6*, 630-41. DOI PubMed PMC
140. Tu, J.; Min, J.; Song, Y.; et al. A wireless patch for the monitoring of C-reactive protein in sweat. *Nat. Biomed. Eng.* **2023**, *7*, 1293-306. DOI PubMed PMC
141. Wang, B.; Zhao, C.; Wang, Z.; et al. Wearable aptamer-field-effect transistor sensing system for noninvasive cortisol monitoring. *Sci. Adv.* **2022**, *8*, eabk0967. DOI PubMed PMC
142. Zhang, X.; Tang, Y.; Wu, H.; Wang, Y.; Niu, L.; Li, F. Integrated aptasensor array for sweat drug analysis. *Anal. Chem.* **2022**, *94*, 7936-43. DOI
143. Zhang, X.; Zhang, J.; Cai, Y.; et al. Integrated electrochemical aptasensor array toward monitoring anticancer drugs in sweat. *Anal. Chem.* **2024**, *96*, 4997-5005. DOI
144. Fu, J.; Wang, Y.; Ding, Y.; et al. Wearable ring sensor for monitoring biomarkers of atherosclerosis in sweat. *Talanta* **2025**, *287*, 127608. DOI
145. Huang, C.; Li, D.; Liu, J.; et al. A flexible aptameric graphene field-effect nanosensor capable of automatic liquid collection/filtering for cytokine storm biomarker monitoring in undiluted sweat. *Adv. Funct. Mater.* **2023**, *34*, 2309447. DOI
146. Gao, Y.; Nguyen, D. T.; Yeo, T.; et al. A flexible multiplexed immunosensor for point-of-care *in situ* wound monitoring. *Sci. Adv.* **2021**, *7*, eabg9614. DOI
147. Huang, C.; Yang, W.; Wang, H.; et al. Flexible/regenerative nanosensor with automatic sweat collection for cytokine storm biomarker detection. *ACS. Nano.* **2024**, *18*, 21198-210. DOI
148. Gao, W.; Ota, H.; Kiriya, D.; Takei, K.; Javey, A. Flexible electronics toward wearable sensing. *Acc. Chem. Res.* **2019**, *52*, 523-33. DOI
149. Chen, S.; Qiao, Z.; Niu, Y.; et al. Wearable flexible microfluidic sensing technologies. *Nat. Rev. Bioeng.* **2023**, *1*, 950-71. DOI
150. Xu, Y.; Ye, Z.; Zhao, G.; et al. Phase-separated porous nanocomposite with ultralow percolation threshold for wireless bioelectronics. *Nat. Nanotechnol.* **2024**, *19*, 1158-67. DOI PubMed PMC
151. Eiler, J.; Hansen, D.; Bingöl, B.; Hansen, K.; Heikenfeld, J.; Thormann, E. *In vitro* evaluation of skin adhesives during perspiration. *Int. J. Adhes. Adhes.* **2020**, *99*, 102574. DOI
152. Si, Y.; Li, C.; Hu, J.; Zhang, C.; Dong, Z. Bioinspired superwetting open microfluidics: from concepts, phenomena to applications. *Adv. Funct. Mater.* **2023**, *33*, 2301017. DOI
153. Sun, Y.; Wang, J.; Lu, Q.; et al. Stretchable and smart wettable sensing patch with guided liquid flow for multiplexed *in situ* perspiration analysis. *ACS. Nano.* **2024**, *18*, 2335-45. DOI
154. He, X.; Xu, T.; Gu, Z.; et al. Flexible and superwettable bands as a platform toward sweat sampling and sensing. *Anal. Chem.* **2019**, *91*, 4296-300. DOI
155. Yang, H.; Ji, S.; Chaturvedi, I.; et al. Adhesive biocomposite electrodes on sweaty skin for long-term continuous electrophysiological monitoring. *ACS. Mater. Lett.* **2020**, *2*, 478-84. DOI
156. Yuan, Q.; Fang, H.; Wu, X.; et al. Self-adhesive, biocompatible, wearable microfluidics with erasable liquid metal plasmonic hotspots for glucose detection in sweat. *ACS. Appl. Mater. Interfaces.* **2023**, *16*, 66810-8. DOI
157. Choi, Y.; Jin, P.; Lee, S.; et al. All-printed chip-less wearable neuromorphic system for multimodal physicochemical health monitoring. *Nat. Commun.* **2025**, *16*, 5689. DOI PubMed PMC
158. Lu, Y.; Yang, G.; Wang, S.; et al. Stretchable graphene-hydrogel interfaces for wearable and implantable bioelectronics. *Nat. Electron.* **2023**, *7*, 51-65. DOI
159. Sonner, Z.; Wilder, E.; Gaillard, T.; Kasting, G.; Heikenfeld, J. Integrated sudomotor axon reflex sweat stimulation for continuous sweat analyte analysis with individuals at rest. *Lab. Chip.* **2017**, *17*, 2550-60. DOI
160. Li, S.; Li, C.; Wang, Y.; Li, H.; Xia, F. Re-engineering electrochemical aptamer-based biosensors to tune their useful dynamic range via distal-site mutation and allosteric inhibition. *Anal. Chem.* **2020**, *92*, 13427-33. DOI
161. Singh, N. K.; Chung, S.; Chang, A.; Wang, J.; Hall, D. A. A non-invasive wearable stress patch for real-time cortisol monitoring using a pseudoknot-assisted aptamer. *Biosens. Bioelectron.* **2023**, *227*, 115097. DOI
162. Downs, A. M.; Plaxco, K. W. Real-time, *in vivo* molecular monitoring using electrochemical aptamer based sensors: opportunities and challenges. *ACS. Sens.* **2022**, *7*, 2823-32. DOI
163. Ogden, N. E.; Kurnik, M.; Parolo, C.; Plaxco, K. W. An electrochemical scaffold sensor for rapid syphilis diagnosis. *Analyst* **2019**, *144*, 5277-83. DOI PubMed PMC
164. Kang, D.; Parolo, C.; Sun, S.; Ogden, N. E.; Dahlquist, F. W.; Plaxco, K. W. Expanding the scope of protein-detecting electrochemical DNA “scaffold” sensors. *ACS. Sens.* **2018**, *3*, 1271-5. DOI PubMed PMC

165. Ma, J.; Zhu, J.; Li, J.; Yang, Y. Design of a cost-effective inverted tetrahedral DNA nanostructure - based interfacial probe for electrochemical biosensing with enhanced performance. *Microchem. J.* **2021**, *168*, 106455. DOI
166. Lin, M.; Wan, H.; Zhang, J.; Wang, Q.; Hu, X.; Xia, F. Electrochemical DNA sensors based on MoS_2-AuNPs for polynucleotide kinase activity and inhibition assay. *ACS. Appl. Mater. Interfaces.* **2020**, *12*, 45814-21. DOI
167. Lai, R. Y. Folding- and dynamics-based electrochemical DNA sensors. In *Enzymes as Sensors*; Methods in Enzymology, Vol. 589; Elsevier, 2017; pp 221-52. DOI
168. Shen, Q.; Fan, M.; Yang, Y.; Zhang, H. Electrochemical DNA sensor-based strategy for sensitive detection of DNA demethylation and DNA demethylase activity. *Anal. Chim. Acta.* **2016**, *934*, 66-71. DOI
169. Idili, A.; Amodio, A.; Vidonis, M.; Feinberg-somerson, J.; Castronovo, M.; Ricci, F. Folding-upon-binding and signal-on electrochemical DNA sensor with high affinity and specificity. *Anal. Chem.* **2014**, *86*, 9013-9. DOI PubMed PMC
170. Luo, X.; Du, F.; Wu, Y.; Gao, L.; Li, X. Electrochemical DNA sensor for determination of p53 tumor suppressor gene incorporating gold nanoparticles modification. *Chin. J. Anal. Chem.* **2013**, *41*, 1664-8. DOI
171. Li, H.; Li, S.; Dai, J.; et al. High frequency, calibration-free molecular measurements *in situ* in the living body. *Chem. Sci.* **2019**, *10*, 10843-8. DOI
172. Li, H.; Dauphin-ducharme, P.; Ortega, G.; Plaxco, K. W. Calibration-free electrochemical biosensors supporting accurate molecular measurements directly in undiluted whole blood. *J. Am. Chem. Soc.* **2017**, *139*, 11207-13. DOI PubMed PMC
173. Lee, T.; Chen, L.; Wang, E.; Wang, C.; Lin, Y.; Chen, W. Development of an electrochemical immunosensor for detection of cardiac troponin I at the point-of-care. *Biosensors* **2021**, *11*, 210. DOI PubMed PMC
174. Feng, X.; Gan, N.; Lin, S.; et al. Ratiometric electrochemiluminescent aptasensor array for antibiotic based on internal standard method and spatial-resolved technique. *Sensor. Actuat. B-Chem.* **2016**, *226*, 305-11. DOI
175. Chen, Z.; Wang, Y.; Du, X.; Sun, J.; Yang, S. Temperature-alternated electrochemical aptamer-based biosensor for calibration-free and sensitive molecular measurements in an unprocessed actual sample. *Anal. Chem.* **2021**, *93*, 7843-50. DOI
176. Du, Y.; Lim, B. J.; Li, B.; Jiang, Y. S.; Sessler, J. L.; Ellington, A. D. Reagentless, ratiometric electrochemical DNA sensors with improved robustness and reproducibility. *Anal. Chem.* **2014**, *86*, 8010-6. DOI PubMed PMC
177. Leung, K. K.; Downs, A. M.; Ortega, G.; Kurnik, M.; Plaxco, K. W. Elucidating the mechanisms underlying the signal drift of electrochemical aptamer-based sensors in whole blood. *ACS. Sens.* **2021**, *6*, 3340-7. DOI PubMed PMC
178. Verrinder, E.; Gerson, J.; Leung, K.; Kippin, T. E.; Plaxco, K. W. Dual-frequency, ratiometric approaches to EAB sensor interrogation support the calibration-free measurement of specific molecules i*n vivo*. *ACS. Sens.* **2024**, *9*, 3205-11. DOI
179. Downs, A. M.; Gerson, J.; Leung, K. K.; Honeywell, K. M.; Kippin, T.; Plaxco, K. W. Improved calibration of electrochemical aptamer-based sensors. *Sci. Rep.* **2022**, *12*, 5535. DOI PubMed PMC
180. Zupančič, U.; Jolly, P.; Estrela, P.; Moschou, D.; Ingber, D. E. Graphene enabled low-noise surface chemistry for multiplexed sepsis biomarker detection in whole blood. *Adv. Funct. Mater.* **2021**, *31*, 2010638. DOI
181. Torrente-rodríguez, R. M.; Lukas, H.; Tu, J.; et al. SARS-CoV-2 RapidPlex: a graphene-based multiplexed telemedicine platform for rapid and low-cost COVID-19 diagnosis and monitoring. *Matter* **2020**, *3*, 1981-98. DOI PubMed PMC
182. Cui, F.; Yue, Y.; Zhang, Y.; Zhang, Z.; Zhou, H. S. Advancing biosensors with machine learning. *ACS. Sens.* **2020**, *5*, 3346-64. DOI
183. Xue, Y.; Ji, W.; Jiang, Y.; Yu, P.; Mao, L. Deep learning for voltammetric sensing in a living animal brain. *Angew. Chem. Int. Ed.* **2021**, *60*, 23777-83. DOI
184. Ali, M.; Naeem, F.; Tariq, M.; Kaddoum, G. Federated learning for privacy preservation in smart healthcare systems: a comprehensive survey. *IEEE. J. Biomed. Health. Inform.* **2023**, *27*, 778-89. DOI
185. Jiang, C.; Wang, G.; Hein, R.; Liu, N.; Luo, X.; Davis, J. J. Antifouling strategies for selective *in vitro* and *in vivo* sensing. *Chem. Rev.* **2020**, *120*, 3852-89. DOI
186. Sabaté Del Río, J.; Henry, O. Y. F.; Jolly, P.; Ingber, D. E. An antifouling coating that enables affinity-based electrochemical biosensing in complex biological fluids. *Nat. Nanotechnol.* **2019**, *14*, 1143-9. DOI
187. Jaffer, I.; Fredenburgh, J.; Hirsh, J.; Weitz, J. Medical device-induced thrombosis: what causes it and how can we prevent it? *J. Thromb. Haemost.* **2015**, *13*, S72-81. DOI
188. Weber, M.; Steinle, H.; Golombek, S.; et al. Blood-contacting biomaterials: *in vitro* evaluation of the hemocompatibility. *Front. Bioeng. Biotechnol.* **2018**, *6*, 99. DOI
189. Khatoon, Z.; Mctiernan, C. D.; Suuronen, E. J.; Mah, T.; Alarcon, E. I. Bacterial biofilm formation on implantable devices and approaches to its treatment and prevention. *Heliyon* **2018**, *4*, e01067. DOI PubMed PMC
190. Caldara, M.; Belgiovine, C.; Secchi, E.; Rusconi, R. Environmental, microbiological, and immunological features of bacterial biofilms associated with implanted medical devices. *Clin. Microbiol. Rev.* **2022**, *35*, e00221-20. DOI PubMed PMC
191. Samant, P. P.; Prausnitz, M. R. Mechanisms of sampling interstitial fluid from skin using a microneedle patch. *Proc. Natl. Acad. Sci. U.S.A.* **2018**, *115*, 4583-8. DOI PubMed PMC

192. Kolluru, C.; Williams, M.; Yeh, J. S.; Noel, R. K.; Knaack, J.; Prausnitz, M. R. Monitoring drug pharmacokinetics and immunologic biomarkers in dermal interstitial fluid using a microneedle patch. *Biomed. Microdevices.* **2019**, *21*, 14. DOI PubMed PMC
193. Gromov, P.; Gromova, I.; Olsen, C. J.; et al. Tumor interstitial fluid - a treasure trove of cancer biomarkers. *BBA-Proteins. Proteom.* **2013**, *1834*, 2259-70. DOI
194. Wiig, H.; Swartz, M. A. Interstitial fluid and lymph formation and transport: physiological regulation and roles in inflammation and cancer. *Physiol. Rev.* **2012**, *92*, 1005-60. DOI
195. Min, J.; Tu, J.; Xu, C.; et al. Skin-interfaced wearable sweat sensors for precision medicine. *Chem. Rev.* **2023**, *123*, 5049-138. DOI PubMed PMC
196. Yang, D. S.; Ghaffari, R.; Rogers, J. A. Sweat as a diagnostic biofluid. *Science* **2023**, *379*, 760-1. DOI
197. Sempionatto, J. R.; Lasalde-Ramírez, J. A.; Mahato, K.; Wang, J.; Gao, W. Wearable chemical sensors for biomarker discovery in the omics era. *Nat. Rev. Chem.* **2022**, *6*, 899-915. DOI PubMed PMC
198. Yang, Y.; Gao, W. Wearable and flexible electronics for continuous molecular monitoring. *Chem. Soc. Rev.* **2019**, *48*, 1465-91. DOI
199. Malon, R. S. P.; Sadir, S.; Balakrishnan, M.; Córcoles, E. P. Saliva-based biosensors: noninvasive monitoring tool for clinical diagnostics. *Biomed. Res. Int.* **2014**, *2014*, 1-20. DOI PubMed PMC
200. Sterzenbach, T.; Helbig, R.; Hannig, C.; Hannig, M. Bioadhesion in the oral cavity and approaches for biofilm management by surface modifications. *Clin. Oral. Investig.* **2020**, *24*, 4237-60. DOI PubMed PMC
201. Qin, S.; Jie, Z.; Chen, L.; et al. Real-time monitoring of daunorubicin pharmacokinetics with nanoporous electrochemical aptamer-based sensors *in vivo*. *Sensor. Actuat. B-Chem.* **2024**, *411*, 135710. DOI
202. Booth, M. A.; Erdal, M. K.; Larson, M.; et al. Pilot phase clinical trial of a wearable, electrochemical aptamer-based patch for continuous drug concentration measurement. *Nat. Biotechnol.* **2026**, 3010. DOI
203. He, Z.; Duan, H.; Zeng, J.; et al. Perovskite retinomorphic image sensor for embodied intelligent vision. *Sci. Adv.* **2025**, *11*, eads2834. DOI PubMed PMC